

**SYNTHESIS OF ZEOLITE SODIUM Y DISPERSED IN  
LEAD TREE WOOD**



**A Thesis Submitted in Partial Fulfillment of Requirements for the  
Degree of Master of Science in Chemistry  
Suranaree University of Technology  
Academic Year 2020**

การสังเคราะห์ซีโอไลต์โซเดียมวายเป็นผงในไม้อัด



วิทยานิพนธ์นี้เป็นส่วนหนึ่งของการศึกษาตามหลักสูตรปริญญาวิทยาศาสตรมหาบัณฑิต  
สาขาวิชาเคมี  
มหาวิทยาลัยเทคโนโลยีสุรนารี  
ปีการศึกษา 2563

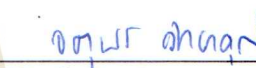
**SYNTHESIS OF ZEOLITE SODIUM Y DISPERSED IN  
LEAD TREE WOOD**

Suranaree University of Technology has approved this thesis submitted in partial fulfillment of the requirements for a Master's Degree.

Thesis Examining Committee

  
\_\_\_\_\_  
(Prof. Dr. James R. Ketudat-Cairns)

Chairperson

  
\_\_\_\_\_  
(Prof. Dr. Jatuporn Wittayakun)

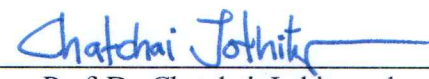
Member (Thesis Advisor)

  
\_\_\_\_\_  
(Assoc. Prof. Dr. Sanchai Prayoonpokarach)

Member (Thesis Co-Advisor)

  
\_\_\_\_\_  
(Dr. Pongtanawat Khemthong)

Member (Thesis Co-Advisor)

  
\_\_\_\_\_  
(Assoc. Prof. Dr. Chatchai Jothityangkoon)

Vice Rector for Academic Affairs  
and Quality Assurance

  
\_\_\_\_\_  
(Prof. Dr. Santi Maensiri)

Dean of Institute of Science

ปณต ครีกรระโทก : การสังเคราะห์ซีโอไลต์โซเดียมวายเป็นวัสดุกระจายตัวภายในไม้กระถิน  
(SYNTHESIS OF ZEOLITE SODIUM Y DISPERSED IN LEAD TREE WOOD).

อาจารย์ที่ปรึกษา : ศาสตราจารย์ ดร.จตุพร วิทยาคุณ, 70 หน้า.

ซีโอไลต์โซเดียมวายเป็นวัสดุอูมิโนซิลิเกตซึ่งใช้ประโยชน์อย่างแพร่หลายในกระบวนการอุตสาหกรรมหลายอย่าง ส่วนใหญ่ซีโอไลต์โซเดียมวายเป็นรูปผง ซึ่งเมื่อจำเป็นต้องแยกออกจากระบบ จะซึ่มาก ดังนั้นงานนี้จึงเสนอการสังเคราะห์ซีโอไลต์โซเดียมวายเป็นวัสดุกระจายตัวในไม้ โดยเลือกไม้กระถินมาใช้เนื่องจากเป็นพืชโตไวและมีมากในประเทศไทย งานวิจัยนี้ศึกษา 3 ปัจจัยในการเกิดผลึกของซีโอไลต์โซเดียมวายเป็นวัสดุกระจายตัวในไม้ ได้แก่ การลดความสูงของไม้ การใช้รังสีอัลตราโซนิก และการรีฟลักซ์ไม้ด้วยกรด หลังการสังเคราะห์ จะระบุเอกลักษณ์ตัวอย่างด้วยเทคนิค XRD SEM และ TGA ตัวอย่างที่ไม่ได้ใช้ปัจจัยทั้ง 3 อย่าง โดยใช้ไม้สูง 0.5 เซนติเมตร จะเกิดซีโอไลต์โซเดียมฟิภายในไม้กระถิน เมื่อสังเคราะห์โดยลดความสูงของไม้ และการใช้รังสีอัลตราโซนิก เพื่อให้สารตั้งต้นแพร่เข้าไปกลางไม้ได้เร็วขึ้น พบว่ายังเกิดซีโอไลต์โซเดียมฟิภายในไม้กระถิน ในขณะที่การสังเคราะห์โดยใช้ไม้ที่รีฟลักซ์ด้วยกรดจะได้ซีโอไลต์โซเดียมวายเป็นผลึก เนื่องจากการใช้รังสีอัลตราโซนิกช่วยขยายรูพรุนของไม้ ทำให้การแพร่ของสารตั้งต้นภายในไม้กระถินได้ดีขึ้น อัตราส่วนเจลภายในไม้กระถินจึงเหมาะสมต่อการสังเคราะห์ซีโอไลต์โซเดียมวายเป็นผลึก ดังนั้นสภาวะการทดลองที่ได้ซีโอไลต์โซเดียมวายเป็นวัสดุกระจายตัวภายในไม้กระถินคือใช้ไม้รีฟลักซ์ ตกผลึกที่ 90°C เป็นเวลา 24 ชั่วโมง และซีโอไลต์ที่ได้มีอนุภาคขนาด 2 ไมโครเมตรอย่างสม่ำเสมอ มีลักษณะทางสัณฐานวิทยาเป็นผลึกแบบโพลิฮีดรอล

สาขาวิชาเคมี

ปีการศึกษา 2563

ลายมือชื่อนักศึกษา ปณต ครีกรระโทก

ลายมือชื่ออาจารย์ที่ปรึกษา จตุพร วิทยาคุณ

PANOT KRUKKRATOKE : SYNTHESIS OF ZEOLITE SODIUM Y  
DISPERSED IN LEAD TREE WOOD. THESIS ADVISOR : PROF.  
JATUPORN WITTAYAKUN, Ph.D. 70 PP.

ZEOLITE SODIUM Y/ FAU/ ULTRASOUND/ REFLUX/ LEAD TREE WOOD/  
HYDROTHERMAL

Zeolite NaY is a crystalline aluminosilicate material which widely used in various industrial processes. Since zeolite NaY is mostly in powder form, the separation process is slow. This work offers an approach to synthesize zeolite NaY dispersed in a wood to solve the problem. Lead tree wood is chosen because it is a fast-growing tree which is abundant in Thailand. This research studies three parameters in the synthesis: reducing the wood height, applying ultrasonic radiation and using wood refluxed in acid. The samples are characterized by XRD, SEM, and TG analysis. The first sample from Lead tree wood with 0.5 cm in a height without acid refluxing and sonication produces zeolite NaP in the wood. After reducing of wood height and applying ultrasonic radiation, the phase of zeolite is still NaP. Refluxing in acid expands the pore width of the wood and improve the diffusion of precursor into the wood. Gel composition inside the wood is suitable for zeolite NaY synthesis. The suitable condition to produce pure phase of zeolite NaY inside the wood is obtained with refluxed Lead tree wood and crystallization at 90°C for 24 h. The obtained zeolite has uniform polyhedral morphology particle with the size about 2  $\mu\text{m}$ .

School of Chemistry

Student's Signature ปณต ครุคราตอก

Academic Year 2020

Advisor's Signature ดร. จตุพร วิฑวณ

## ACKNOWLEDGEMENTS

First of all, I would like to express my gratitude to Prof. Dr. Jatuporn Wittayakun, my advisor, for his patience, support and help throughout all two years. He gave me everything that he could including motivation, guidance and enthusiasm which are very meaningful for my research. I could not even imagine if I don't have such a perfect professor.

I would like to acknowledge my scholarship, Thailand Graduated Institute of Science and Technology (TGIST, Contract No. SCA-CO-2562-9802-TH), from National Science and Technology Development Agency (NSTDA). I sincerely thank all professors of the School of Chemistry for their suggestions and consultation. I also thank Suranaree University of Technology (SUT). Thank all members of catalysis group at SUT and everyone for everything.

Last but not least, my appreciative thanks are my parents and other family members for their unconditional love, encouragement, and support in all situations in my whole life.

Panot Krukkratoke

# CONTENTS

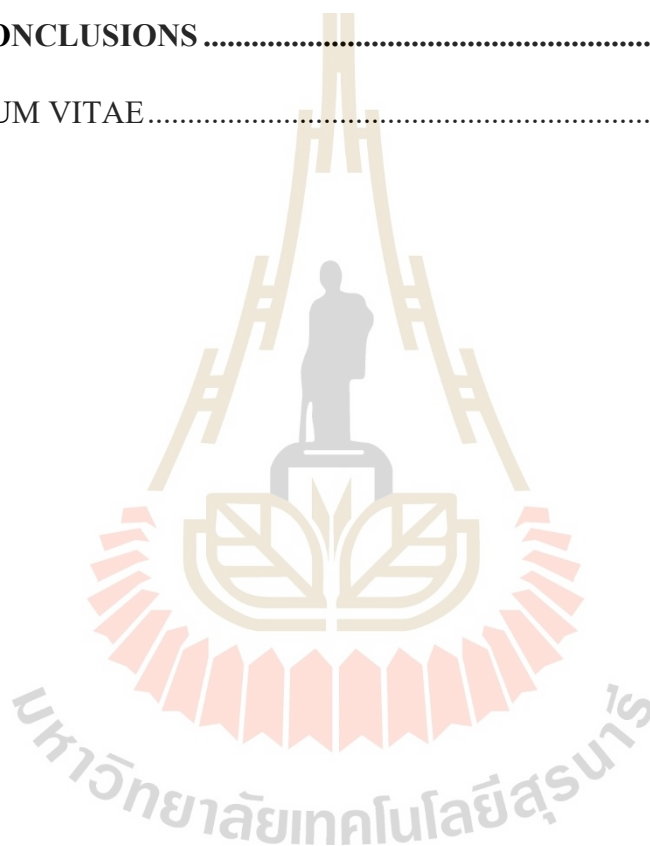
	<b>Page</b>
ABSTRACT IN THAI.....	I
ABSTRACT IN ENGLISH .....	II
ACKNOWLEDGEMENTS.....	IV
CONTENTS.....	V
LIST OF TABLES.....	VIII
LIST OF FIGURES .....	IX
<b>CHAPTER</b>	
<b>I INTRODUCTION .....</b>	<b>1</b>
1.1 Introduction.....	1
1.2 Objectives .....	3
1.3 References.....	3
<b>II LITERATURE REVIEW .....</b>	<b>6</b>
2.1 Lead tree wood.....	6
2.2 Synthesis of zeolite NaY.....	8
2.3 Synthesis of zeolite/wood composite.....	12
2.4 Adjustment of experimental conditions.....	15
2.4.1 Wood refluxing.....	15
2.4.2 Reducing of wood height .....	16

## CONTENTS (Continued)

		<b>Page</b>
	2.4.3 Ultrasonic radiation-assisted for zeolite NaY synthesis.....	16
	2.5 References.....	17
<b>III</b>	<b>EXPERIMENTAL.....</b>	<b>23</b>
	3.1 Chemicals.....	23
	3.2 Synthesis of zeolite NaY/lead tree wood composite.....	24
	3.2.1 Preparation of lead tree wood.....	24
	3.2.2 Synthesis of NaY/LW composite .....	25
	3.3 Material characterization .....	27
	3.4 References.....	27
<b>IV</b>	<b>RESULTS AND DISCUSSION .....</b>	<b>29</b>
	4.1 XRD pattern and SEM images of Lead tree wood .....	29
	4.2 XRD pattern and SEM images of LW-NR-0.5.....	30
	4.3 Effect of wood refluxing.....	37
	4.4 Effect of ultrasonic radiation .....	39
	4.5 Effect of wood height .....	41
	4.6 Effect of wood height with wood refluxing and ultrasonic radiation .....	45
	4.7 Zeolite powder outside the Lead tree wood.....	49

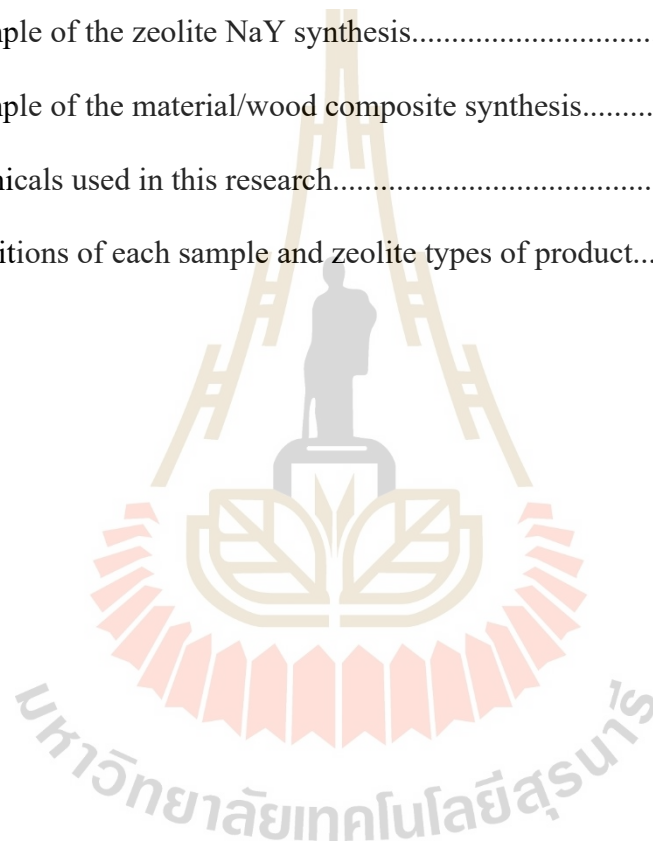
**CONTENTS (Continued)**

	<b>Page</b>
4.8 Thermal Stability and %zeolite by TGA .....	63
4.9 References.....	66
<b>V CONCLUSIONS .....</b>	<b>69</b>
<b>CURRICULUM VITAE.....</b>	<b>71</b>



## LIST OF TABLES

Table	Page
1.1	Example of the material/wood composite synthesis.....3
2.1	Example of the zeolite NaY synthesis.....9
2.2	Example of the material/wood composite synthesis.....13
3.1	Chemicals used in this research.....23
4.1	Conditions of each sample and zeolite types of product.....66



## LIST OF FIGURES

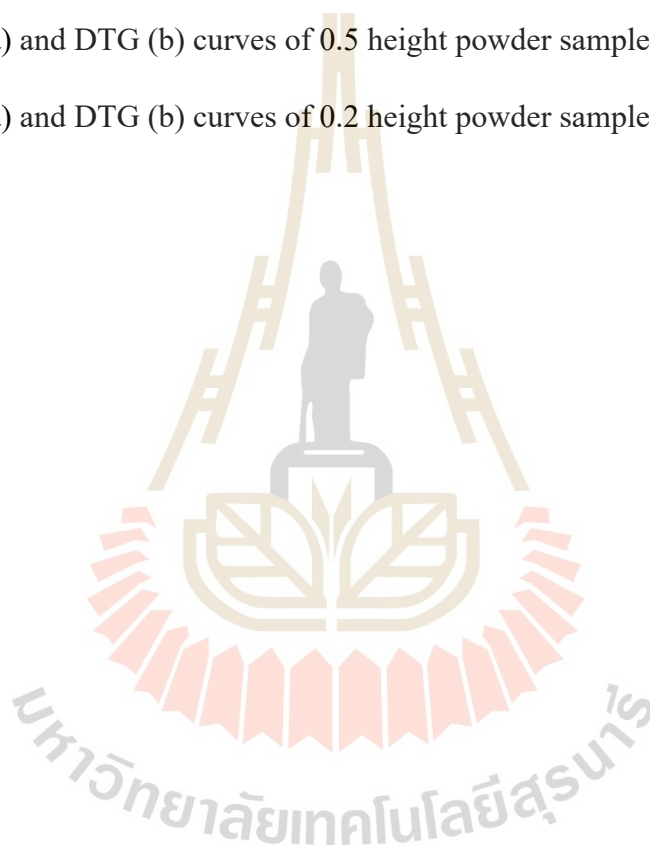
<b>Figure</b>	<b>Page</b>
1.1 SEM images of LW .....	2
2.1 Picture of Lead tree and SEM image of lead tree wood.....	7
2.2 Structure of double 6 rings, sodalite cage, and zeolite NaY .....	8
2.3 SEM images of untreated and refluxed lead tree wood.....	16
3.1 0.5 height LW and 0.2 height LW .....	24
3.2 Scheme of synthetic conditions in this research and the name of the samples ..	26
4.1 XRD pattern of dried LW.....	29
4.2 SEM images of LW with different magnification: 100x(a), 500x(b), and 1000x .....	30
4.3 XRD pattern of LW, LW-NR-0.5, zeolite NaY from IZA, and zeolite NaP from IZA .....	31
4.4 SEM images of LW-NR-0.5 .....	32
4.5 XRD pattern of zeolite NaY from IZA, and Pow-LW-NR-0.5.....	34
4.6 SEM images of Pow-LW-NR-0.5 .....	35
4.7 XRD pattern of LW-R-0.5 and LW-NR-0.5 .....	38
4.8 SEM images of LW-R-0.5.....	38
4.9 XRD patterns of LW-NR-So-0.5 and LW-R-So-0.5.....	40
4.10 SEM images of LW-NR-So-0.5 .....	40

## LIST OF FIGURES (Continued)

<b>Figure</b>	<b>Page</b>
4.11 XRD pattern of LW-NR-0.5 and LW-NR-0.2.....	43
4.12 XRD pattern of LW-NR-0.5 and LW-NR-0.2 .....	43
4.13 SEM images of LW-NR-0.2.....	44
4.14 XRD pattern of LW-R-So-0.2, LW-NR-So-0.2, and LW-R-0.2.....	46
4.15 SEM images of LW-R-0.2.....	47
4.16 SEM images of LW-NR-So-0.2.....	48
4.17 SEM images of LW-R-So-0.2.....	49
4.18 XRD pattern of 0.5 height powder samples .....	51
4.19 XRD pattern of 0.2 height powder samples .....	52
4.20 SEM images of Pow-LW-R-0.5 .....	54
4.21 SEM images of Pow-LW-NR-So-0.5.....	55
4.22 SEM images of Pow-LW-R-So-0.5.....	56
4.23 SEM images of Pow-LW-NR-0.2 .....	57
4.24 SEM images of Pow-LW-R-0.2 .....	58
4.25 SEM images of Pow-LW-NR-So-0.2.....	60
4.26 SEM images of Pow-LW-R-So-0.2.....	61
4.27 SEM images of powder samples .....	62
4.28 TGA (a) and DTG (b) curves of 0.5 height sample.....	64

## LIST OF FIGURES (Continued)

Figure	Page
4.29 TGA (a) and DTG (b) curves of 0.2 height sample.....	64
4.30 TGA (a) and DTG (b) curves of 0.5 height powder sample.....	64
4.31 TGA (a) and DTG (b) curves of 0.2 height powder sample.....	65



# CHAPTER I

## INTRODUCTION

Zeolite NaY is a crystalline aluminosilicate material with the molecular formula of  $\text{Na}_x[(\text{AlO}_2)_x(\text{SiO}_2)_y] \cdot n\text{H}_2\text{O}$ . The framework of zeolite NaY has a faujasite (FAU) structure containing periodic supercages with a diameter of 1.3 nm and four windows with a diameter of 0.74 nm (Guisnet and Gilson, 2002).

Zeolite NaY is used in various industrial processes, including catalysis (Krisnandi et al., 2019) and adsorption (Rongchapo et al., 2013; Rongchapo et al., 2017; Keawkumay et al., 2019; and Kulawong et al., 2020). Zeolite NaY in those situations is normally in powder form which takes time in the separation and produces waste such as filter paper and syringe filter. To ease the separation, zeolite NaY could be dispersed in biomass with large pores.

Valtchev et al. (2004) mixed ZSM-5 precursor with pieces of *Equisetum arvense* leaves and stems to produce ZSM-5/*Equisetum arvense* wood composite with 30-60 mm size. This interesting synthesis is called “dual templating” method. More examples of the material/wood composite are summarized in table 1. However, the supporting materials in Table 1.1, are fragile and easily degrade under simple laboratory operations. This method could be further improved by using a wood that is hard and abundant in Thailand. The interest in this work is Lead tree wood (*Leucaena*

*leucocephala de Wit*). The SEM image of LW in Figure 1 shows wide pores which could serve as hosts of zeolite particles (Pimsuta et al., 2016).

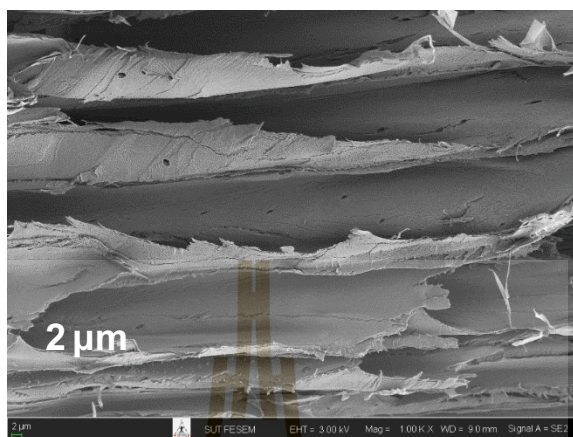


**Figure 1.1** SEM images of LW (Pimsuta et al., 2016).

**Table 1.1** Example of the material/wood composite synthesis.

Material	Supporting material		Ref.
	Name	Type	
ZSM-5	<i>Equisetum arvense</i>	Leaves and stems	Valtchev et al., 2004
ZSM-5	Corn	Stems	Krishnamurthy, 2015
ZSM-5	Rice	Husk	Morawala et al., 2019
ZSM-5 and	<i>Luffa cylindrica</i>	Fruit	Zampieri et al., 2006
Silicalite-1	sponges		
Silicalite-1	27 palm fibers	Stems	Xu et al., 2010
Zeolite Beta	<i>Equisetum arvense</i>	Leaves and stems	Valtchev et al., 2004

## 1.2 Objectives

The objectives of this thesis are (i) to prepare a pure phase of zeolite NaY in a Lead tree wood (NaY/LW) composite by a hydrothermal method and (ii) to understand in the synthesis including applying sonication, refluxing the wood by hydrochloric acid, and reducing of the wood height.

## 1.3 References

- Guisnet, M., and Gilson, J. P. (2002). Zeolites for cleaner technologies. **London: Imperial College Press.**
- Keawkumay, C., Rongchapo, W., Sosa, N., Suthirakun, S., Koleva, I. Z., Aleksandrov, H. A., Vayssilov, G. N., and Wittayakun, J. (2019). Paraquat adsorption on NaY zeolite at various Si/Al ratios: A combined experimental and computational study. **Materials Chemistry and Physics.** 238: 121824.
- Krishnamurthy, M. (2015). Hierarchically structured MFI zeolite monolith prepared using agricultural waste as solid template. **Microporous and Mesoporous Materials.** 221: 23-31.
- Krisnandi, Y. K., Saragi, I. R., Sihombing, R., Ekananda, R., Sari, I. P., Griffith, B. E., and Hanna, J. V. (2019). Synthesis and characterization of crystalline NaY-zeolite from Belitung kaolin as catalyst for n-hexadecane cracking. **Crystals.** 9(8): 404.
- Kulawong, S., Chanlek, N., and Osakoo, N. (2020). Facile synthesis of hierarchical structure of NaY zeolite using silica from cogon grass for acid blue 185

removal from water. **Journal of Environmental Chemical Engineering**. 8(5): 104114.

Morawala, D., Dalai, A., and Maheria, K. (2019). Rice husk mediated synthesis of meso-ZSM-5 and its application in the synthesis of n-butyl levulinate. **Journal of Porous Materials**. 26(3): 677-686.

Pimsuta, M. (2016). **Nickel phosphide on activated carbon for hydrodeoxygenation of palm oil**, Ph.D. Thesis, Suranaree University of Technology, Nakhon Ratchasima, Thailand.

Rongchapo, W., Keawkumay, C., Osakoo, N., Deekamwong, K., Chanlek, N., Prayoonpokarach, S., and Wittayakun, J. (2017). Comprehension of paraquat adsorption on faujasite zeolite X and Y in sodium form. **Adsorption Science and Technology**. 36(1-2): 684-693.

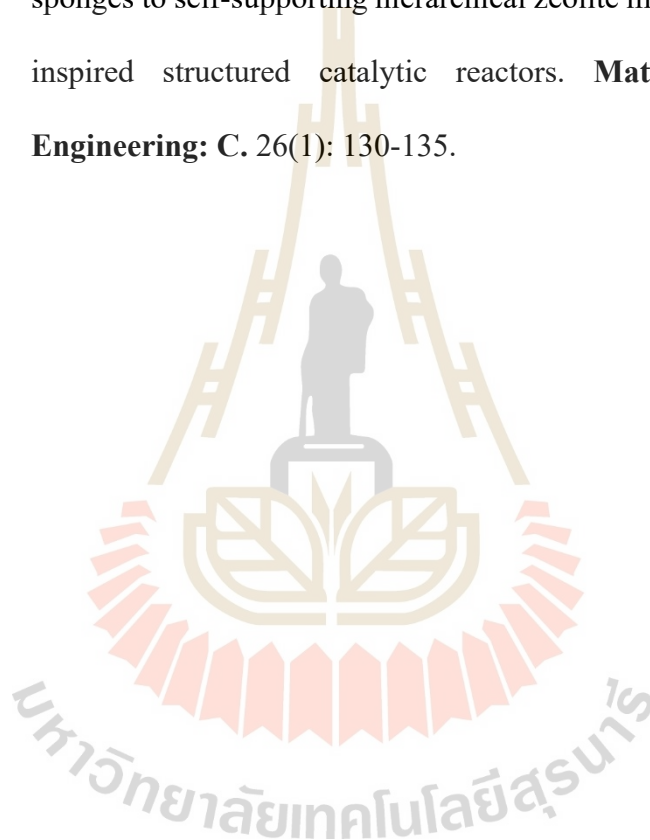
Rongchapo, W., Sophiphun, O., Rintramee, K., Prayoonpokarach, S., and Wittayakun, J. (2013) Paraquat adsorption on porous materials synthesized from rice husk silica. **Water Science and Technology**. 68(4): 863-869.

Valtchev, V. P., Smaih, M., Faust, Faust, A., and Vidal, L. (2004). *Equisetum arvense* templating of zeolite beta macrostructures with hierarchical porosity. **Chemistry of Materials**. 16(7): 1350-1355.

Valtchev, V., Smaih, M., Faust, A. C., and Vidal, L. (2004). Dual templating function of *Equisetum Arvense* in the preparation of zeolite macrostructures. **Studies in Surface Science and Catalysis**. 154(Part A): 588-592.

Xu, J., Yao, J., Zeng, C., Zhang, L., and Xu, N. (2010). Preparation of binderless honeycomb silicalite-1 monolith by using bundled palm fibers as template. **Journal of Porous Materials**. 17: 329-334.

Zampieri, A., Mabande, G., Selvam, T., Schwieger, W., Rudolph, A., Hermann, R., Sieber, H., and Greil, P. (2006). Biotemplating of *Luffa cylindrica* sponges to self-supporting hierarchical zeolite macrostructures for bio-inspired structured catalytic reactors. **Materials Science and Engineering: C**. 26(1): 130-135.



## CHAPTER II

### LITERATURE REVIEW

This chapter provides the literature review of basic information of Lead tree wood, synthesis of zeolite NaY, and synthesis of zeolite/wood composite. The adjustment of experimental conditions including wood refluxing, reducing of wood height, and applying sonication for zeolite NaY synthesis is reviewed.

#### 2.1 Lead tree wood

Lead tree or *Leucaena Leucocephala* (Figure 2.1a) is abundant in Nakhon Ratchasima province. It is a small shrub or tree, 3-10 m height, and not deciduous. Lead tree is a fast-growing. Some parts of the lead tree are edible. The leaves, top pods and young seeds are used as food for cattle, goats, sheep and chickens. Some farmers plant it to protect from wind and make use of the shade for crops such as tea and coffee. Moreover, the Lead tree wood is a heavy hardwood (Nazri et al., 2012). Consequently, some people use the stems as a fuel in household. When the lead tree wood is more than the human need, farmers often eliminate them by cutting and burning.

Lead tree wood consists of cellulose (55.87%), hemicellulose (34.73%), and lignin (18.63%) (Amini et al., 2017). The lead tree is a dicotyledon plant with a

wide diameter of xylem and phloem about  $10\ \mu\text{m}$ , this is wider than the zeolite NaY size which is about  $200\ \text{nm} - 5\ \mu\text{m}$  (Figure 2.1b).

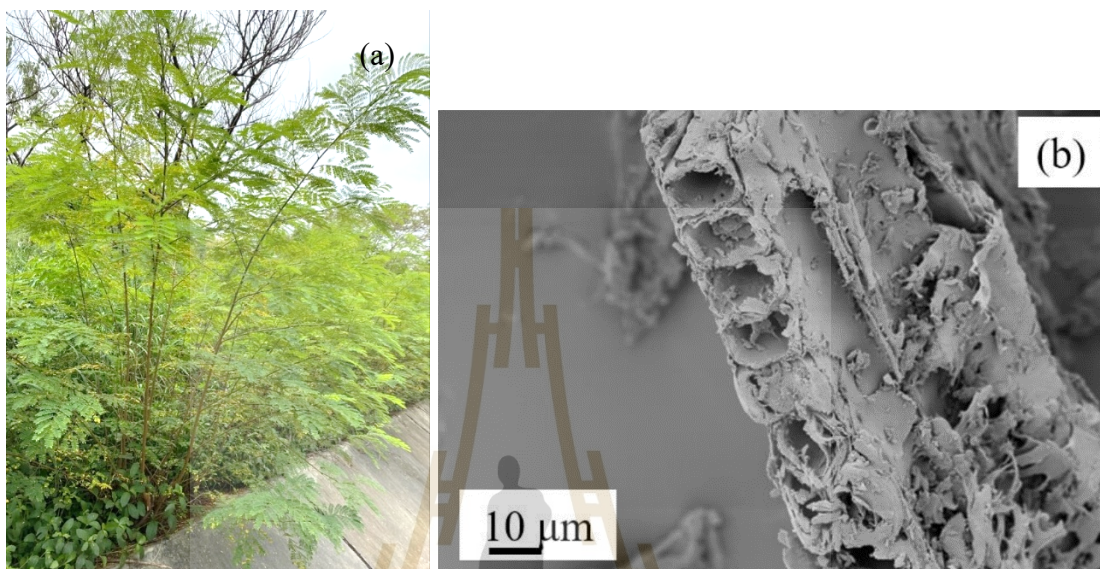


**Figure 2.1** Figure of (a) Lead tree and (b) SEM image of lead tree wood (Pimsuta et al., 2016).

## 2.2 Synthesis of zeolite NaY

Zeolites NaY possesses a faujasite framework containing double 6 rings (Figure 2.2a) and sodalite cage (Figure 2.2b), which result in periodic supercages with a diameter of  $1.3\ \text{nm}$  and four windows with a diameter of  $0.74\ \text{nm}$  (Figure 2.2c).

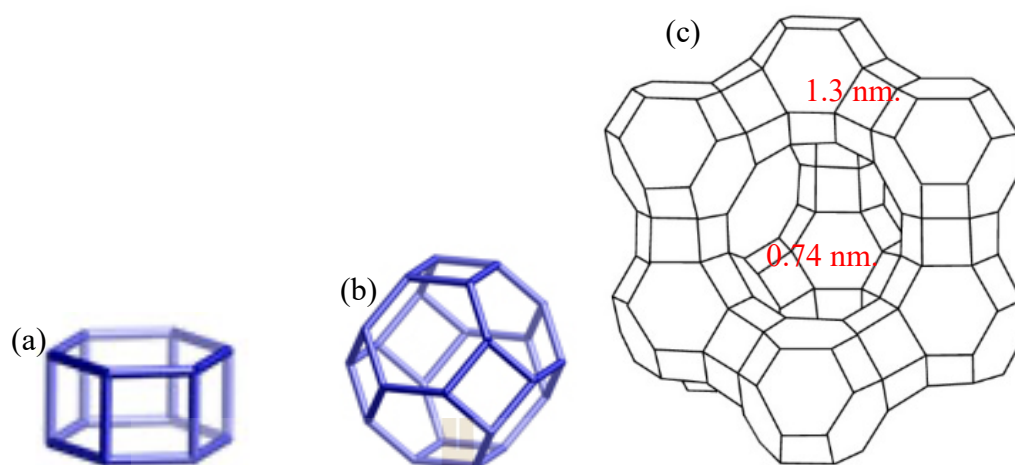


**Figure 2.2** Structure of (a) double 6 rings, (b) sodalite cage, and (c) zeolite NaY (Lutz, 2014).

In a general synthesis from IZA, zeolite NaY is synthesized by hydrothermal method from an overall gel with molar ratio of  $4.62\text{Na}_2\text{O} : 1\text{Al}_2\text{O}_3 : 10\text{SiO}_2 : 180\text{H}_2\text{O}$ . The overall gel is prepared by mixing the seed gel ( $10.67\text{Na}_2\text{O} : 1\text{Al}_2\text{O}_3 : 10\text{SiO}_2 : 180\text{H}_2\text{O}$ ) and feedstock gel ( $4.3\text{Na}_2\text{O} : 1\text{Al}_2\text{O}_3 : 10\text{SiO}_2 : 180\text{H}_2\text{O}$ ). Then, overall gel is aged at room temperature for 24 h and treated in hydrothermal process at  $100^\circ\text{C}$  for 24 h.

Table 2.1 shows examples of zeolite NaY synthesis including the use of template, assistance of sonication, and assistance of microwave, and conventional hydrothermal method. The use of the template produces a uniform zeolite supercage (Khalifah et al., 2018 and Wang et al., 2010), but it was not considered a green method because it requires additional chemicals. The assistance of sonication and microwave reduce the crystallization time (Bunmai et al., 2018; Wang et al., 2010; Jing, 2009; Panzarella et al., 2007; Katsuki et al., 2001).

In the case of conventional methods, Wittayakun et al. (2008) synthesized pure phase of zeolite NaY from rice husk silica. The overall molar gel composition ( $4.62\text{Na}_2\text{O}: 1\text{Al}_2\text{O}_3: 10\text{SiO}_2: 180\text{H}_2\text{O}$ ) was prepared by mixing a feedstock gel into a seed gel, followed by aging for 24 h at room temperature and hydrothermal process at  $90^\circ\text{C}$  for 24 h.

**Table 2.1** Examples of the zeolite NaY synthesis.

Overall gel molar composition				Hydrothermal		Special synthetic method	Si/Al ratio	Ref.
$\text{Na}_2\text{O}$	$\text{Al}_2\text{O}_3$	$\text{SiO}_2$	$\text{H}_2\text{O}$	Temp ( $^\circ\text{C}$ )	Time (h)			
3.5	1	4	200	100	22		4	Shariatini et al., 2018
				100	24	Using Bangka Belitung kaolin as a $\text{SiO}_2$ and $\text{Al}_2\text{O}_3$ source	3.8	Krisnandi et al., 2018
9	1	6	249	100	48	Using CTABr as a template Using kaolin as a $\text{SiO}_2$ source, calcined $550^\circ\text{C}$ , 1 h		Khalifah et al., 2018

**Table 2.1** Examples of the zeolite NaY synthesis (Continued).

Overall gel molar composition				Hydrothermal		Special synthetic method	Si/Al ratio	Ref.
Na <sub>2</sub> O	Al <sub>2</sub> O <sub>3</sub>	SiO <sub>2</sub>	H <sub>2</sub> O	Temp (°C)	Time (h)			
4.62	1	10	180	100	24	Using SiO <sub>2</sub> from cogon grass with 250 GHz microwave and power 300 W	2.98	Bunmai et al., 2018
4	1	8	200	90	12	Overall gel composition = 4 : 1 : 8 : 200 : 20 of [BmimBF <sub>4</sub> ] with microwave – assisted, using metakaolinite as a SiO <sub>2</sub>	5.02	Wang et al., 2010
				100	24	Synthesis in nonionic emulsion system		Zhang et al., 2010
9.6	1	14.4	334	60	48	Aging for 24 h with stirring at 650 rpm and further aging for 24 h at 38°C	2.5	Huang et al., 2010
2.22-2.8	1	6.0-7.0	96-140	100	28	Using metakaolinite as a SiO <sub>2</sub> , aging time = 6.5-22 h	>2.5	Qiang et al., 2010

**Table 2.1** Examples of the zeolite NaY synthesis (Continued).

Overall gel molar composition				Hydrothermal		Special synthetic method	Si/Al ratio	Ref.
Na <sub>2</sub> O	Al <sub>2</sub> O <sub>3</sub>	SiO <sub>2</sub>	H <sub>2</sub> O	Temp (°C)	Time (h)			
4	1	8	200	90	12	Using metakaolin as a SiO <sub>2</sub> source, ultrasonic assisted for 2 h at 40°C	5.12	Jing, 2009
4.62	1	10	180	90	24	Using SiO <sub>2</sub> from rice husk, two step (aging feedstock gel for 24 h, at room temp)		Wittayakun et al., 2008
4	1	8	140			Using 2.45 GHz microwave, in situ SAXS and WAXS study		Panzarella et al., 2007
14	1	10	800	100	3	Using microwave assistance with 2.45 GHz, 300 W		Katsuki et al., 2001
4	1	10.6	130	98	21	Using kaolinite as a SiO <sub>2</sub> and Al <sub>2</sub> O <sub>3</sub> source, hydrothermal with refluxing and stirring	3	Basaldella et al., 1993

### 2.3 Synthesis of zeolite/wood composite

Zeolite NaY in powder form is difficult to separate from an experimental system. Therefore, forming large particles can solve the problem. Du et al. (2008) synthesized zeolite NaY with a spherical shape (3-5 mm) by using a turntable granulator and sprayed in the binder solution to form seed crystals. This method provides a uniform and strong particle. Nevertheless, the problem is low contact point (compare with powder form) and high cost from binder and service charge.

The synthesis of material/wood composite is an interesting method to improve the material. This synthesis allows the material to grow in the vascular system. Table 2.2 shows examples of the material/wood composite synthesis. In the past 20 years, ZSM-5 was the most synthesized in a composite method with the part of plants such as leaves and stems of *Equisetum arvense* (Valtchev et al., 2004), fruit of *Luffa cylindrica* sponges (Zampieri et al., 2006), stems of corn (Krishnamurthy et al., 2016), and rice husk (Morawala et al., 2019). In the case of *Equisetum arvense*, the plant is fragile and easy to degrade. If strong plants are used, the application of this material may be more efficient. In the case of corn stem, the advantage of this template is the tangible pellet, which looks ready to use.

**Table 2.2** Examples of the material/wood composite synthesis.

Material	Supporting material		Ref.
	Name	Type	
ZSM-5	<i>Equisetum arvense</i>	Leaves and stems	Valtchev et al., 2004
ZSM-5	Corn	Stems	Krishnamurthy et al., 2016
ZSM-5	Rice	Husk	Morawala et al., 2019
ZSM-5 and Silicalite-1	<i>Luffa cylindrica</i> sponges	Fruit	Zampieri et al., 2006
Silicalite-1	27 palm fibers	Stems	Xu et al., 2010
SiO <sub>2</sub> hollow microspheres	Rape pollen grain by bees	Flower	Cao et al., 2009
macro/meso porous SiO <sub>2</sub>	Manchurian ash and mango linin		Qu et al., 2010
Zeolite Beta	<i>Equisetum arvense</i>	Leaves and stems	Valtchev et al., 2004
NiO/ZnO nanocomposite	Poplar tree	Leaves	Zeng et al., 2020
NaX zeolite	Silicalite honeycomb monolith	Cuttlebone	Li et al., 2009

In addition, silica/supporting material composites were interested for the synthesis such as flower of rape pollen grain (Cao et al., 2009), stems of 27 palm fibers (Xu et al., 2010), and Manchurian ash and mango linin (Qu et al., 2010). In the case of 27 palm fibers, this template is a filament that is not suitable for zeolite NaY applications.

There are some research about zeolite synthesis with a solid template including ZSM-5 on the surface of rice husk (Morawala et al., 2019), Silicalite-1 and ZSM-5 in the pore of *Luffa cylindrica* sponges (Zampieri et al., 2006), and ZSM-5 on the surface and in the pore of corn stem pith (Krishnamurthy et al., 2016). Those studies show that zeolite could be synthesized inside the wood.

In the case of FAU zeolite such as zeolite NaX and zeolite NaY, there are no reports on synthesis in plant as a supporting material. Li et al. (2009) synthesized NaX zeolite in silicalite honeycomb monolith which was produced from the cuttlebone of giant cuttlefish (*Sepia apama*). The synthesis was done by mixing all chemicals for NaX zeolite in the same container with the silicalite honeycomb monolith. The gel molar composition was  $\text{NaAlO}_2: 4\text{SiO}_2: 16\text{NaOH}: 325\text{H}_2\text{O}$ . Although, this monolith provided a uniform pore and strong template, it is not as abundant as plant. Consequently, it may not be suitable for the synthesis in a pilot scale.

All the research above has a similar synthesis method, that is, mixing the ingredients together followed by adding the supporting material. After that, the mixtures were treated with hydrothermal methods under various conditions (temperature, time, refluxing, and aging). Up to date, there are no reports about synthetic zeolite NaY/wood composite. This composite is interesting because zeolite NaY has a large surface area and highly stable. Furthermore, zeolite NaY has many applications including catalysis, separation, and adsorption.

There are several reports that zeolite NaP is produced in the synthesis of zeolite NaY (Wittayakun et al., 2008; Zhang et al., 2010; Li et al., 2011; Tavasoli et al., 2014; Bunmai et al., 2018). The addition of water to the synthesis system affects the solubility of the aluminum source and the hydrolysis process of various inorganic

elements (Xu et al., 2007). In addition, reducing the water content of the initial hydrogel accelerates the crystal growth process and improves the synthesis of zeolite membranes (Shirazian et al., 2014). It means that a small amount of water or a high concentration of sodium hydroxide can dissolve sodium silicate quickly. So, sodium silicate can react quickly with sodium aluminate, which results in a fast crystallization process. The resulting crystals are zeolite NaP. In short, zeolite NaP has a faster crystallization rate than zeolite NaY.

In the case of zeolite NaY/LW composite, the big concern is that the wood template can adsorb water, resulting in less water content in the vascular system. It means that the crystallization rate in the pore will be faster than the outside and the end of the pore, which leads to zeolite NaP. If zeolite NaY is not produced in the pore, wood refluxing, reducing wood height, and sonication will be applied.

## **2.4 Adjustment of experimental conditions**

### **2.4.1 Wood refluxing**

It is well known that lead tree wood contains cellulose, hemicellulose, lignin, and other components. Some components can be cleaned by water but some components cannot. Refluxing the wood with strong acid can remove some components. Furthermore, wood refluxing can expand the pore of wood about 2  $\mu\text{m}$  in diameter (Figure 2.3), resulting in better diffusion of chemical for zeolite NaY synthesis.

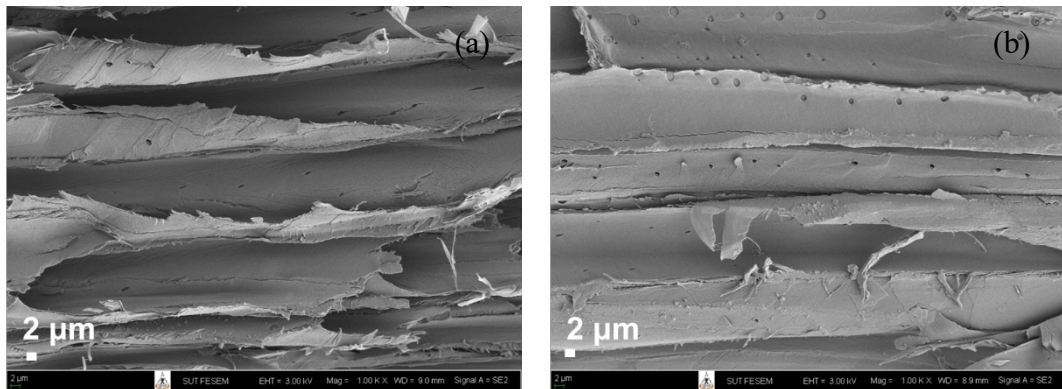


**Figure 2.3** SEM images of (a) untreated and (b) refluxed lead tree wood.

#### 2.4.2 Reducing of wood height

There are no reviews for wood height reduction. The following are just hypotheses. When the wood template is large, the dispersion of the various mixtures, especially water is poor. Water is a media which carries other chemicals to interact with each other. If the content is not water suitable, it will affect the gel composition. Reducing the wood height could ensure water dispersion throughout the wood.

#### 2.4.3 Applying of sonication for synthesis of wood-zeolite

In 2009, Jing synthesized nano-sized zeolite NaY from metakaolin by hydrothermal method with sonication assistance. They reported that sonication can improve the dispersion of liquid in gel composition. The good dispersion results in the efficient reaction of chemicals. Mohammadnezhad et al. (2017) incorporated poly(methyl methacrylate) (PMMA) and polystyrene (PS) via a sonication method. In the introduction part, they reported that the intense ultrasonic radiation can produce bubbles in liquids, then, the bubbles are grown and collapse. In 2018, Soltani

et al. synthesized Amino-modified MCM-41/poly(vinyl alcohol) nanocomposite by using sonication assistance. They reported that high temperatures and high pressures are produced after bubbles collapse. From the aforementioned, such knowledge can be applied to our work. The mixture in gel composition is easily dispersed inside the wood through high temperatures and high pressures from sonication assistance. Moreover, this higher temperatures and higher pressures can accelerate the dissolution of silica and alumina.

Thus, it is proposed in this research to improve NaY/LW composite from different conditions including wood refluxing, reducing of wood height, and applying sonication. The zeolite both inside and outside the wood will be characterized by X-ray diffraction (XRD), scanning electron microscopy with energy dispersive X-ray spectroscopy (SEM-EDX), thermogravimetric analysis (TGA), and Fourier transform infrared spectrometry (FTIR).

## 2.5 References

- Amini, M. H., Rasat, M. S., Rasat, M., Ahmad, I., Wahab, R., Elham, P., Rahman, W., and Ramle, N. (2017). Chemical composition of small diameter wild *Leucaena leucocephala* species. **ARPJ Journal of Engineering and Applied Sciences**. 12(10): 3196-3173.
- Basaldella, E. I., Bonetto, R., and Tara, J. C. (1993). Synthesis of NaY zeolite on preformed kaolinite spheres. Evolution of zeolite content and textural properties with the reaction time. **Industrial & Engineering Chemistry Research**. 32(4): 751-752.

- Bunmai, K., Osakoo, N., Deekamwong, K., Rongchapo, W., Keawkumay, C., Chanlek, N., Prayoonpokarach, S., and Wittayakun, J. (2018). Extraction of silica from cogon grass and utilization for synthesis of zeolite NaY by conventional and microwave-assisted hydrothermal methods. **Journal of the Taiwan Institute of Chemical Engineers**. 83: 152-158.
- Cao, F., and Li, D. (2009). Morphology-controlled synthesis of SiO<sub>2</sub> hollow microspheres using pollen grain as a biotemplate. **Biomedical Materials (Bristol, England)**. 4: 025009.
- Huang, Y., Wang, K., Dong, D., Li, D., Hill, M., Hill, A., and Wang, H. (2010). Synthesis of hierarchical porous zeolite NaY particles with controllable particle sizes. **Microporous and Mesoporous Materials**. 127(3): 167-175.
- Jing, W. (2009). Ultrasonic assisted synthesis of nano-sized NaY zeolite composite from metakaolin by hydrothermal method. **Asian Journal of Chemistry**. 21(9): 7041-7048.
- Katsuki, H., Furuta, S., and Komarneni, S. (2001). Microwave versus conventional-hydrothermal synthesis of NaY zeolite. **Journal of Porous Materials**. 8(1): 5-12.
- Khalifah, S., Nur Aini, Z., Hayati, E., Aini, N., and Prasetyo, A. (2018). Synthesis and characterization of mesoporous NaY zeolite from natural Blitar's kaolin. **IOP Conference Series: Materials Science and Engineering**. 333(1): 012005.

- Krishnamurthy, M. (2015). Hierarchically structured MFI zeolite monolith prepared using agricultural waste as solid template. **Microporous and Mesoporous Materials**. 221: 23-31.
- Krisnandi, Y., Parmanti, I. Y., Yunarti, R., Sihombing, R., and Saragi, I. R. (2018). Synthesis and characterization of zeolite NaY from kaolin Bangka Belitung with variation of synthesis composition and crystallization time. **Journal of Physics: Conference Series**. 1095(1): 012043.
- Li, G., Singh, R., Li, D., Zhao, C., Liu, L., and Webley, P. A. (2009). Synthesis of biomorphic zeolite honeycomb monoliths with 16 000 cells per square inch. **Journal of Materials Chemistry**. 19(44): 8372-8377.
- Li, J., Chi, Z., and Chen, H. (2011). Synthesis of NaY zeolite molecular sieves from calcined diatomite. **Advanced Materials Research**. PP. 236-238, 362-368.
- Lutz, W. (2014). Zeolite Y: Synthesis, Modification, and Properties—A Case Revisited. **Advances in Materials Science and Engineering**. 2014, 1-20.
- Mohammadnezhad, G., Abad, S., Soltani, R., and Dinari, M. (2017). Study on thermal, mechanical and adsorption properties of amine-functionalized MCM-41/PMMA and MCM-41/PS nanocomposites prepared by ultrasonic irradiation. **Ultrasonics Sonochemistry**. 39(1): 765-773.
- Morawala, D., Dalai, A., and Maheria, K. (2019). Rice husk mediated synthesis of meso-ZSM-5 and its application in the synthesis of n-butyl levulinate. **Journal of Porous Materials**. 26(3): 677-686.

- Nazri, W., Rahman, W., Kasim, J., Nawawi, R., Hamid, H., Sudin, R., and Yunus, N. (2012). Anatomical properties of *Leucaena leucocephala* wood: effects on oriented strand board. **Research Journal of Forestry**. 6: 55-65.
- Panzarella, B., Tompsett, G., Conner, W., and Jones, K. (2007). In situ SAXS/WAXS of zeolite microwave synthesis: NaY, NaA, and beta zeolites. **Chemphyschem : a European journal of chemical physics and physical chemistry**. 8(3): 357-369.
- Pimsuta, M. (2016). **Nickel phosphide on activated carbon for hydrodeoxygenation of palm oil** (Unpublished doctor's dissertation). School of Chemistry Institute of Science Suranaree University of Technology, Nakhon Ratchasima, Thailand.
- Qiang, L., Zhang, Y., Cao, Z., Gao, W., and Cui, L. (2010). Influence of synthesis parameters on the crystallinity and Si/Al ratio of NaY zeolite synthesized from kaolin. **Petroleum Science**. 7: 403-409.
- Qu, F., Lin, H., Wu, X., Li, X., Qiu, S., and Zhu, G. (2010). Bio-templated synthesis of highly ordered macro-mesoporous silica material for sustained drug delivery. **Solid State Sciences**. 12(5): 851-856.
- Shariatnia, Z., and Bagherpour, A. (2018). Synthesis of zeolite NaY and its nanocomposites with chitosan as adsorbents for lead(II) removal from aqueous solution. **Powder Technology**. 338: 744-763.
- Shirazian, S., Ghafarnejad Parto, S., and Ashrafizadeh, S. N. (2013). Effect of water content of synthetic hydrogel on dehydration performance of nanoporous

LTA zeolite membranes. **International Journal of Applied Ceramic Technology**, 11(5): 793-803.

Soltani, R., Dinari, M., and Mohammadnezhad, G. (2018). Ultrasonic-assisted synthesis of novel nanocomposite of poly(vinyl alcohol) and amino-modified MCM-41: A green adsorbent for Cd(II) removal. **Ultrasonics Sonochemistry**. 40(Pt A): 533-542.

Tavasoli, M., Kazemian, H., Sadjadi, S., and Tamizifar, M. (2014). Synthesis and characterization of zeolite NaY using kaolin with different synthesis methods. **Clays and Clay Minerals**. 62(6): 508-518.

Wang, X., and Yan, C. (2010). Synthesis of nano-sized NaY zeolite composite from metakaolin by ionothermal method with microwave assisted. **Inorganic Materials**. 46: 517-521.

Wittayakun, J., Khemthong, P., and Prayoonpokarach, S. (2008). Synthesis and characterization of zeolite NaY from rice husk silica. **Korean Journal of Chemical Engineering**. 25: 861-864.

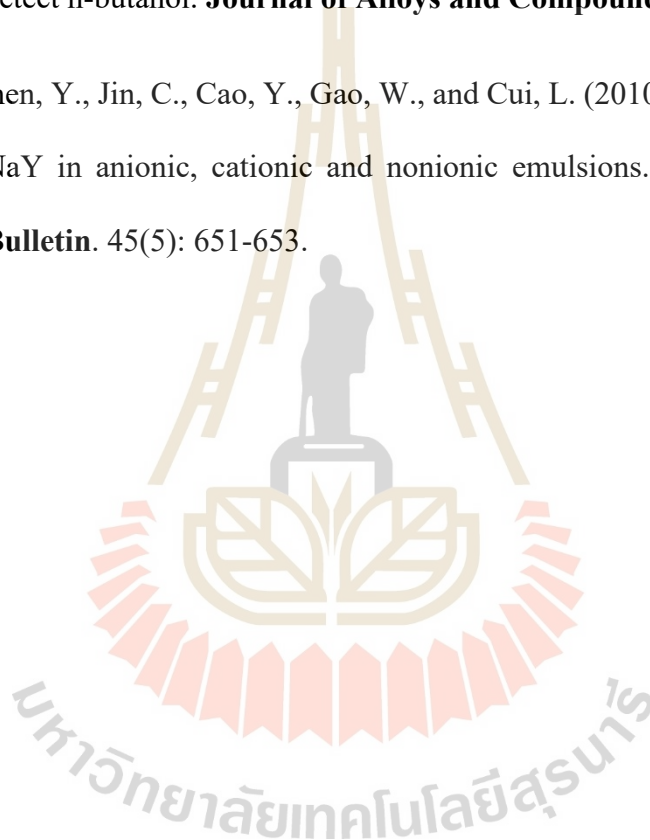
Xu, R., Pang, W., Yu, J., Huo, Q., and Chen, J. (2007). Chemistry of zeolites and related porous materials. **Synthesis and Structure**. New York: John Wiley & Sons, 117-189.

Zampieri, A., Mabande, G., Selvam, T., Schwieger, W., Rudolph, A., Hermann, R., Sieber, H., and Greil, P. (2006). Biotemplating of *Luffa cylindrica* sponges to self-supporting hierarchical zeolite macrostructures for bio-inspired

structured catalytic reactors. **Materials Science and Engineering: C**. 26(1): 130-135.

Zeng, Q., Feng, J., Lin, X., Zhao, Y., Liu, H., Wang, S., Dong, Z., and Feng, W. (2020). One-step facile synthesis of a NiO/ZnO biomorphic nanocomposite using a poplar tree leaf template to generate an enhanced gas sensing platform to detect n-butanol. **Journal of Alloys and Compounds**. 815: 150550.

Zhang, Y., Shen, Y., Jin, C., Cao, Y., Gao, W., and Cui, L. (2010). Synthesis of zeolite NaY in anionic, cationic and nonionic emulsions. **Materials Research Bulletin**. 45(5): 651-653.



## CHAPTER III

### EXPERIMENTAL

#### 3.1 Chemicals

Materials and chemicals used in this research are listed in Table 3.1.

**Table 3.1** Materials and chemicals.

Chemicals	Formula	Content (%)/grade	Suppliers
Lead tree wood	-	-	-
Fumed silica	SiO <sub>2</sub>	99.8%	Sigma-Aldrich
Sodium hydroxide	NaOH	97%	Carlo Erba
Sodium aluminate	NaAlO <sub>2</sub>	99%	Riedel-de Haën®
Hydrochloric acid	HCl	37%	ANaPURE®

## 3.2 Synthesis of zeolite NaY/lead tree wood composite

### 3.2.1 Preparation of lead tree wood

The obtained lead tree wood (LW) was peeled and chopped to the size of 30 cm and dried at 90°C for 96 h in a hot air oven. The dried lead tree wood was separated only 0.75 cm in diameter. After that, the dried lead tree wood was cut to obtain a height of 0.5 cm and 0.2 cm, respectively (Figure 3.1). The cut lead tree wood was dried at 90°C for 24 h in a hot air oven.

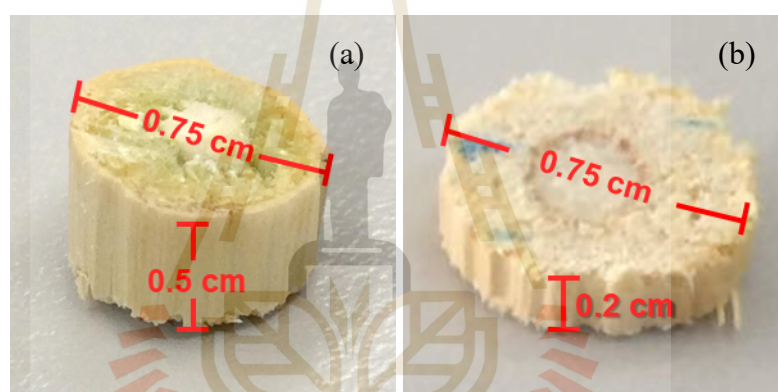


**Figure 3.1** Dried Lead tree wood with the height of (a) 0.5 cm and (b) 0.2 cm.

The lead tree wood was refluxed with a procedure from Bunmai et al. (2018). Briefly, 5.00 g of the wood was refluxed in 67 mL of 3 M HCl at 90°C for 6 h, cooled down, filtered and washed with DI water until the filtrate was neutral. Then, the filtrate was dried at 90°C for 24 h in a hot air oven.

### 3.2.2 Synthesis of NaY/LW composite

NaY/LW composite sample was synthesized with the procedure from Mintova et al. (2002) with an overall gel composition of  $4.62\text{Na}_2\text{O}: 1\text{Al}_2\text{O}_3: 10\text{SiO}_2: 180\text{H}_2\text{O}$ . However, the amount of water was slightly changed to ensure that the wood was completely immersed under the base solution with the same gel composition. Briefly, a seed gel with a gel composition of  $10.57\text{Na}_2\text{O}: 1\text{Al}_2\text{O}_3: 10.56\text{SiO}_2: 332\text{H}_2\text{O}$  was prepared by dissolving 1.00 g of NaOH in 10.00 g of DI water in a centrifuge tube followed by addition 1.00 g of LW to the basic solution. The mixture was capped and aged at room temperature for 24 h. Then, the mixture was transferred to Teflon bottle and 0.4180 g of anhydrous NaAlO<sub>2</sub> (Riedel-de Haën®, 41.383% Na<sub>2</sub>O, 58.604% Al<sub>2</sub>O<sub>3</sub>) was added to the mixture and stirred until homogeneous. After that, 4.7952 g of Na<sub>2</sub>SiO<sub>3</sub> solution was added and the mixture, stirred for 10 min, capped, and aged at room temperature for 24 h.

A feedstock gel with a gel composition of  $4.67\text{Na}_2\text{O}: 1\text{Al}_2\text{O}_3: 10\text{SiO}_2: 158\text{H}_2\text{O}$  was prepared by dissolving 0.0350 g of NaOH in 22.3 g of DI water in a plastic beaker followed by addition 2.7820 g of anhydrous NaAlO<sub>2</sub> to the basic solution and stirred until homogeneous. After that, 30.1881 g of Na<sub>2</sub>SiO<sub>3</sub> solution was added and the mixture was stirred vigorously for 10 min. The feedstock gel was poured to the seed gel and stirred for 10 min, capped, and aged at room temperature for 24 h. The overall gel was crystallized by hydrothermal method at 90°C, for 24 h in a hot air oven. The sample was washed with DI water until neutral. The NaY/LW composite was washed by a sonication bath and the zeolite powder was washed with centrifugation several times at 4000 rpm for 5 min. The NaY/LW composite samples (Figure 3.2) was named LW-NR-X or LW-R-X where NR = not refluxed, R = refluxed and X = height

of LW. The zeolite NaY powder samples was named Pow-LW-NR-X or Pow-LW-R-X.

In the case of applying sonication, the overall gel was sonicated with the procedure from Sosa et al. (2020). Briefly, the overall gel was sonicated immediately after the feedstock gel was poured to the seed gel at an ambient atmosphere with an on-off pulse every five seconds in 30 min using an ultrasonic processor (Sonics Vibra-Cell: VCX 130) with a frequency of 20 kHz and a power of 130 W equipped with a probe size of 6 mm. After that, the overall gel was aged at room temperature for 24 h and crystallized with the same condition. The NaY/LW composite samples (Figure 3.2) was named LW-NR-So-X or LW-R-So-X where So = sonication. The zeolite NaY powder samples was named Pow-LW-NR-So-X or Pow-LW-R-So-X.

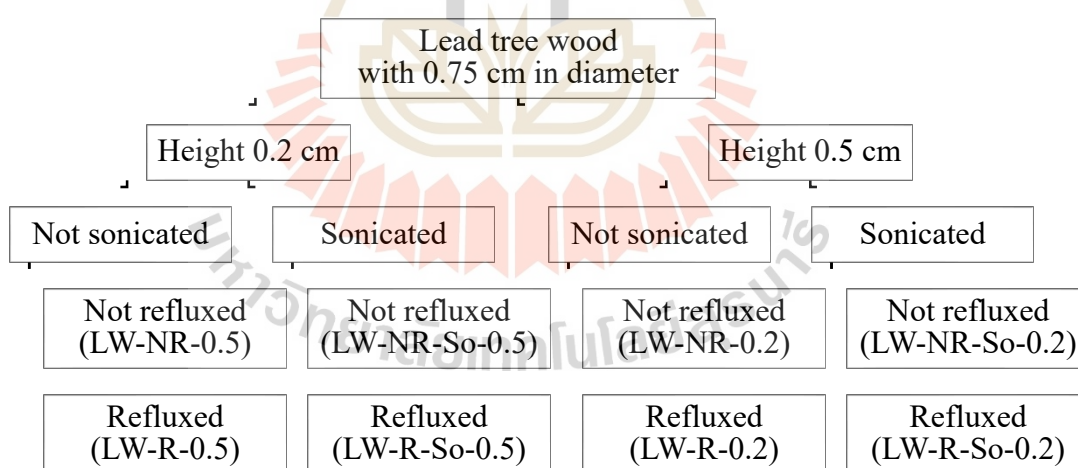


**Figure 3.2** Scheme of synthetic conditions in this research and the name of the samples.

### 3.3 Material characterization

Phases of zeolite was investigated by X-ray diffraction (XRD) on a Bruker D8 ADVANCE with a monochromatic light source Cu K $\alpha$  radiation ( $\lambda = 1.5418$  Å) operated at voltage and current of 40 kV and 30 mA. The samples were analyzed at  $2\theta = 5-50^\circ$  by using scan speed 0.2 s/step and increment 0.02 s/step.

Morphology and particle size of zeolite was analyzed by scanning electron microscopy with energy dispersive X-ray spectroscopy (SEM-EDX, JEOL model JSM-6400) running with an electron beam accelerating voltage of 20 kV, vacuum pressure of  $10^{-4}$  Pa and a tungsten filament. The synthesized samples were spread on a layer of carbon tape with gold or carbon coating.

Phase transition and thermal decomposition of the samples and zeolite NaY weight in the wood was calculated by thermogravimetric analysis (TGA). The TGA was performed by Mettler Toledo model TGA/DSC1 in air zero with flow rate of 50 mL/min at a heating rate of  $10^\circ\text{C}/\text{min}$  up to  $800^\circ\text{C}$ . At  $800^\circ\text{C}$ , assuming that after the wood is burnt out, the remains only consist of zeolite.

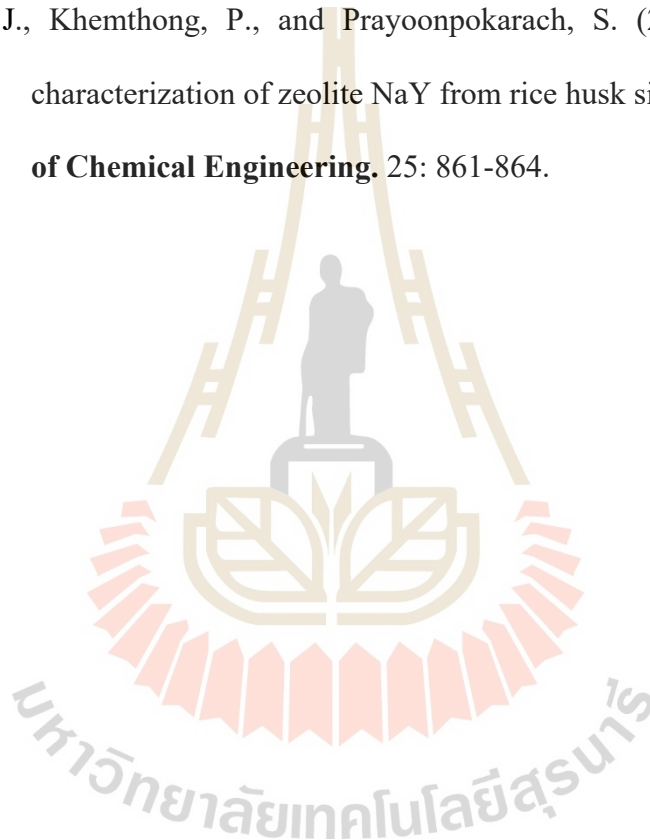
### 3.4 References

Bunmai, K., Osakoo, N., Deekamwong, K., Rongchapo, W., Keawkumay, C., Chanlek, N., Prayoonpokarach, S., and Wittayakun, J. (2018). Extraction of silica from cogon grass and utilization for synthesis of zeolite NaY by conventional and microwave-assisted hydrothermal methods. **Journal of the Taiwan Institute of Chemical Engineers**. 83: 152-158.

Mintova, S. and Lillerud, K. P. (2016) **Verified Syntheses of Zeolitic Materials** (2nd ed.). 156-158. Amsterdam: Elsevier.

Sosa, N., Chanlek, N., and Wittayakun, J. (2020). Facile ultrasound-assisted grafting of silica gel by aminopropyltriethoxysilane for aldol condensation of furfural and acetone. **Ultrasonics Sonochemistry**. 62(1): 104857.

Wittayakun, J., Khemthong, P., and Prayoonpokarach, S. (2008). Synthesis and characterization of zeolite NaY from rice husk silica. **Korean Journal of Chemical Engineering**. 25: 861-864.



## CHAPTER IV

### RESULTS AND DISCUSSION

#### 4.1 XRD pattern and SEM images of Lead tree wood

Lead tree wood (LW) was dissected and analyzed by XRD and SEM. Figure 4.1 shows the XRD pattern of the dried LW and the inset is the wood on the XRD sample holder. The XRD pattern exhibits two peaks at  $14^\circ$  and  $22^\circ$ . These positions are similar to the peaks of cellulose crystal (Li et al., 2011). The broad peaks indicate that it has amorphous nature.

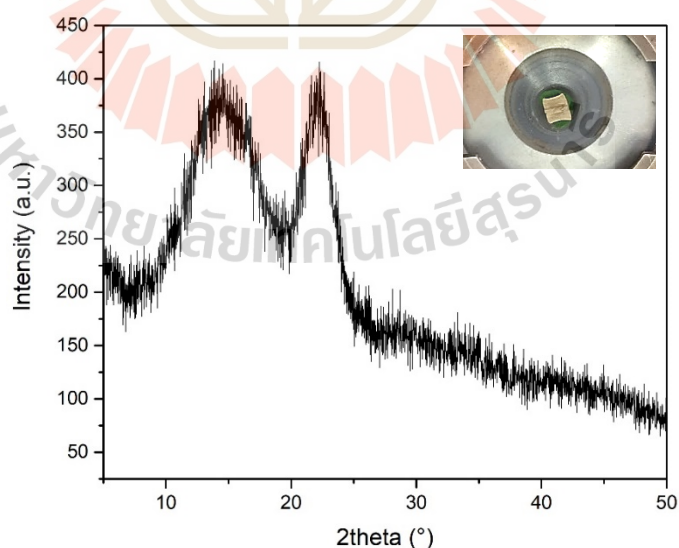


**Figure 4.1** XRD pattern of dried LW.

Figure 4.2 shows the SEM images of dissected LW with different magnification. The inset is the wood on the SEM stub. Figure 4.2a and 4.2b show the fiber of the wood. Figure 4.2c shows the vascular structure with a pore width of about 10  $\mu\text{m}$ . This pore size is similar to the work by Pimsuta (2016).

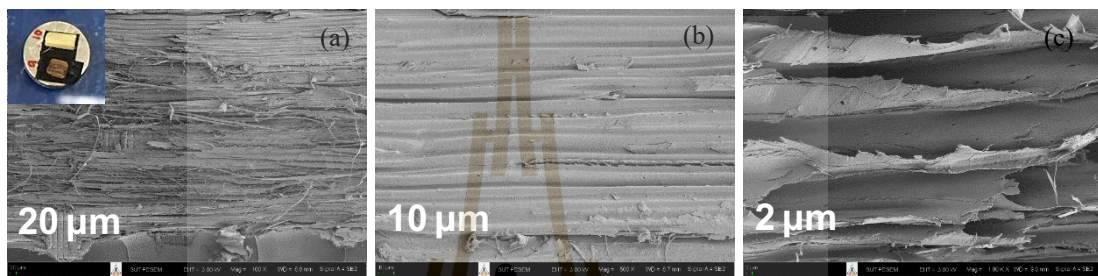


**Figure 4.2** SEM images of LW with different magnification: (a) 100x, (b) 500x, and (c) 1000x.

#### 4.2 XRD pattern and SEM images of LW-NR-0.5

Figure 4.3 shows the XRD pattern of LW-NR-0.5 compared with LW, zeolite NaY and zeolite NaP (Baerlocher and McCusker, 2020). The pattern of LW-NR-0.5 shows characteristics of zeolite NaP and LW. This result shows that zeolite NaP was produced on LW from the gel of NaY by aging at room temperature for 1 day and crystallization at 90°C for 24 h. From the literature, zeolite NaP could be obtained from the gel of NaY under different synthesis conditions. Khabuanchalad et al. (2008) reported that NaP was produced from the gel of NaY by conventional hydrothermal method from two conditions. NaP as an impurity phase was observed when the gel of

NaY was aged at room temperature for 2 days or more, followed by crystallization at 100°C for 1 day. When the aging time was fixed at 1 day, NaP was obtained by crystallization for 2 days or more. Pure phase NaP was obtained from the crystallization of 4 days. Tayraukham et al. (2020) synthesized NaP from the gel of NaY by crystallization at 150°C with conventional and microwave-assisted hydrothermal methods. The crystallization time of the latter method was much shorter, namely, 30-60 minutes.

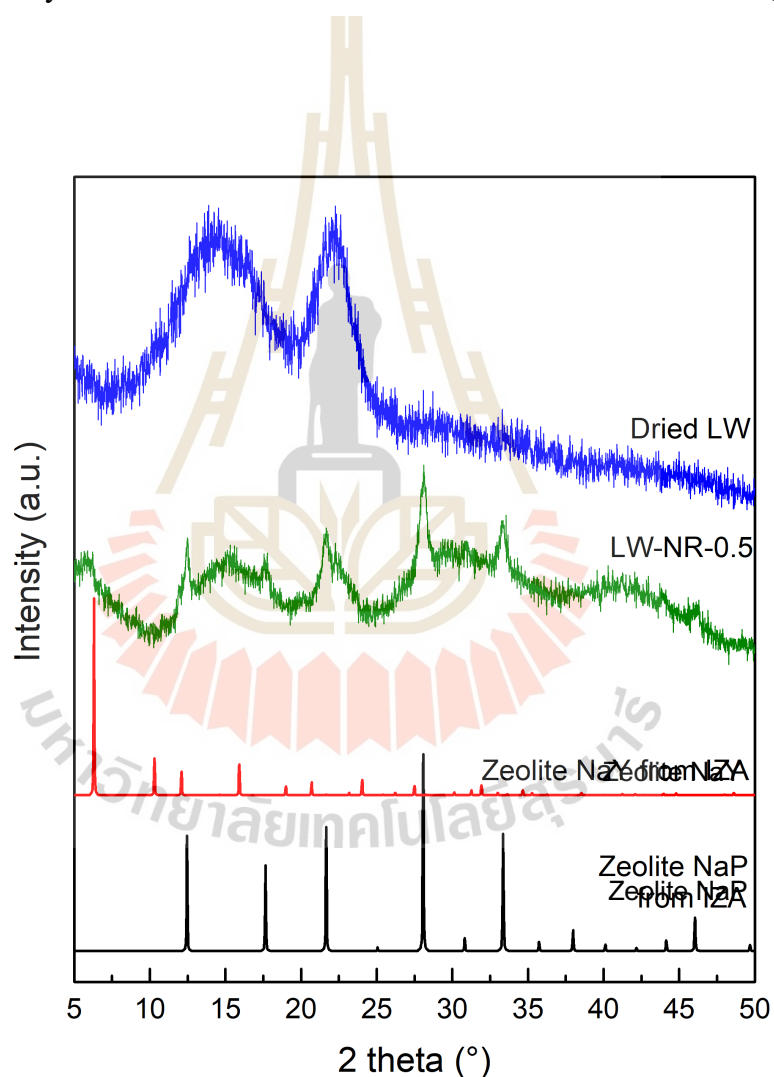


**Figure 4.3** XRD pattern of LW (blue line), LW-NR-0.5 (green line), zeolite NaY (Baerlocher, Ch. and McCusker, L. 2020) (red line), and zeolite NaP (Baerlocher, Ch. and McCusker, L. 2020) (black line).

Figure 4.4 shows the SEM images of LW-NR-0.5. The inset in Figure 4.4a shows the wood on the SEM stub. The SEM images show particles with a uniform size around  $2\ \mu\text{m}$  disperse in the pore of LW. These particles have spherical morphology similar to that of zeolite NaP in the literature (Huo et al., 2012). The zoom-in images (Figure 4.4f-h) show that each particle consists of several small crystals (Figure 4.4b).

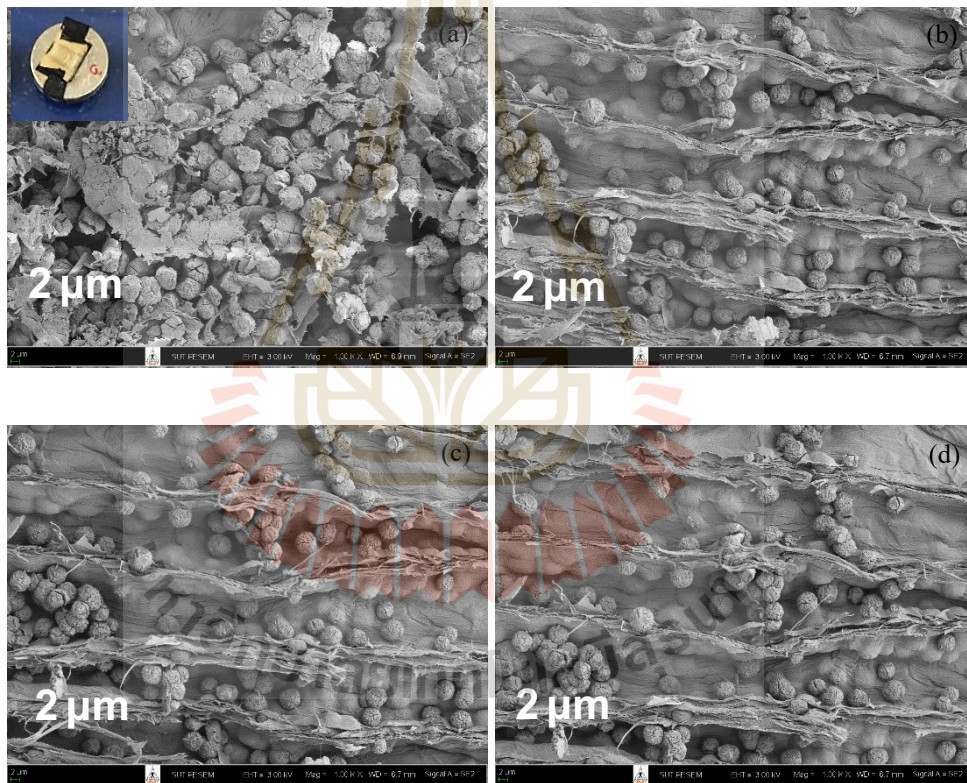


**Figure 4.4** SEM images of LW-NR-0.5.

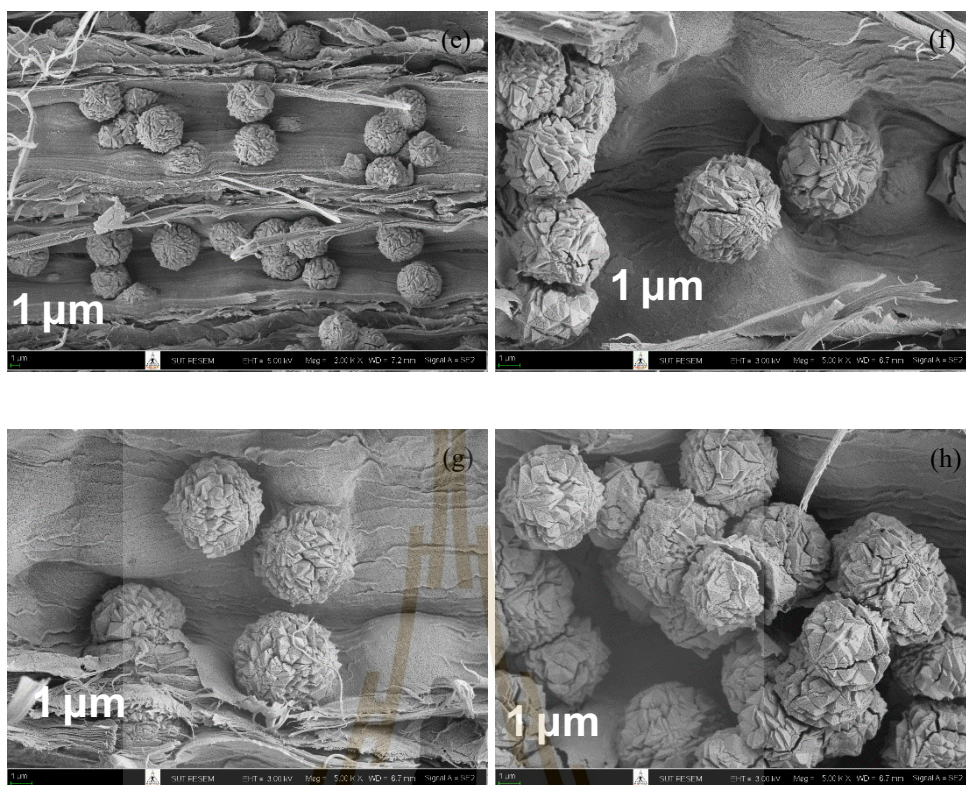
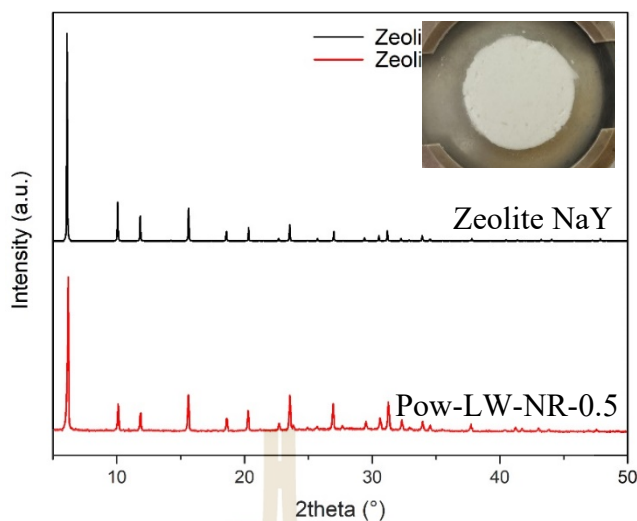


Figure 4.4 SEM images of LW-NR-0.5 (Continued).

Besides the zeolite-containing wood, the powder from the synthesis was characterized by XRD and SEM. Figure 4.5 shows XRD pattern of Pow-LW-NR-0.5 compared with that of NaY from IZA. The inset is the picture of sample powder packed in the XRD holder. The XRD pattern of Pow-LW-NR-0.5 has peak positions similar to NaY.



**Figure 4.5** XRD pattern of zeolite NaY (black line), and Pow-LW-NR-0.5 (red line).

Figures 4.6a-o show SEM images of Pow-LW-NR-0.5. Figure 4.6a shows various particles including wood fragments (1), agglomerated zeolite (2), zeolite in the pores of wood (3). Figure 4.6b-c show the zeolite crystals inside the wood pores. The size of is about 2-3  $\mu\text{m}$ . Figure 4.6d-g displays crystals of the zeolite stuck to the wood or agglomerated with a few crystals or separated from others. Figure 4.6h-o shows crystals with polyhedral morphology and a size about 3  $\mu\text{m}$ . The shape of these crystals are similar to NaY zeolite (Wittayakun et al., 2008). These crystals mix with flaky particles seem to be amorphous. Furthermore, there are round and more-or-less smooth particles that could be amorphous silica. Last but not least, there are spherical particles with wool ball-like morphology with a size of 3-5  $\mu\text{m}$ . These particles are similar to that of zeolite NaP (Huo et al., 2012). However, the amount of zeolite NaP was small and it could not be detected by XRD.

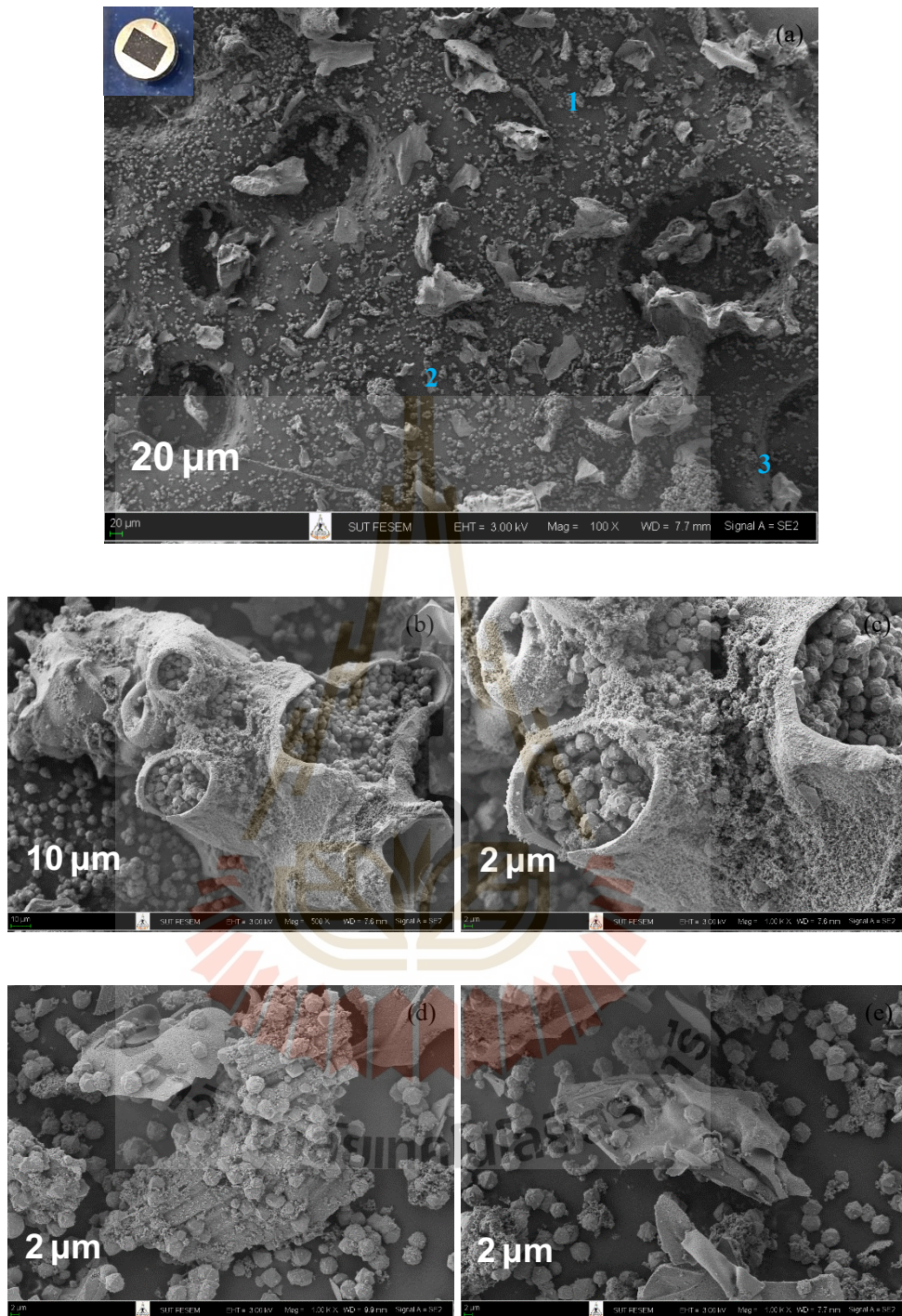


**Figure 4.6** SEM images of Pow-LW-NR-0.5.

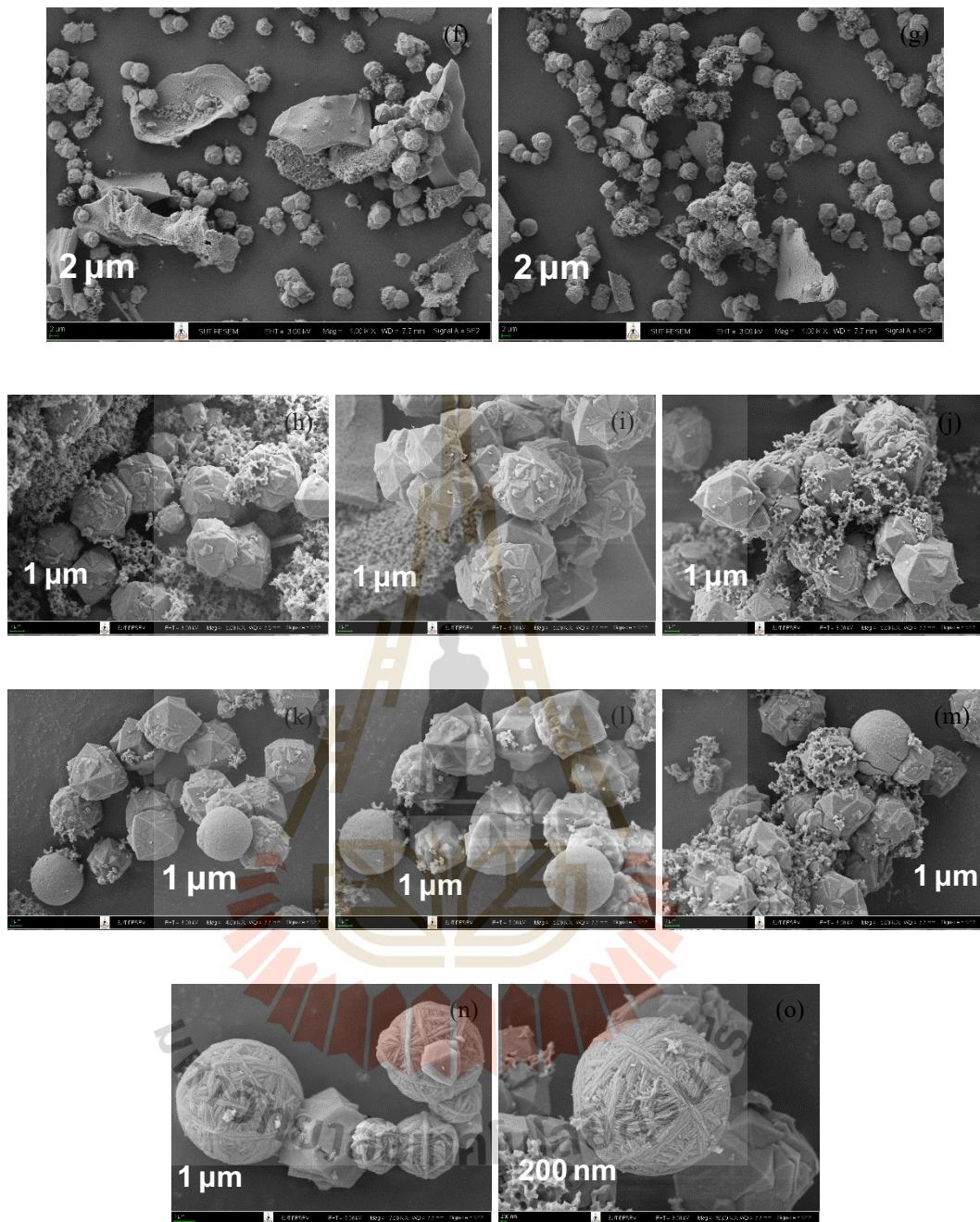


**Figure 4.6** SEM images of Pow-LW-NR-0.5 (Continued).

Shirazian et al. (2013) have explained the formation of NaP from the gel composition of zeolite NaY. Zeolite NaP has a faster crystallization rate than zeolite

NaY. There are two possible explanations in this work. When the wood is mixed with alkaline solution, water can be absorbed by wood. The resulting solution has higher alkalinity which could lead to a faster crystallization. Another possibility is that the roughness in the wood pores serves as nucleation sites for crystallization.

There are three approaches to explore methods to improve the synthesis of zeolite in the wood: refluxing the wood in acid, reducing the wood height and applying sonication. The reasons from each method are discussed in the literature review (2.4 adjustment of experimental conditions). Briefly, the wood was refluxed in 3 M HCl at 90°C for 6 h to clear the pores. It was observed that the wood pore is expanded from 10  $\mu\text{m}$  to 12  $\mu\text{m}$  (Figure 2.3). In the case of reducing of wood height, shorter wood might allow water to disperse throughout the wood more quickly. In the case of sonication assistance, the radiation produces temperature and pressure that can push the precursor to the middle of the wood.

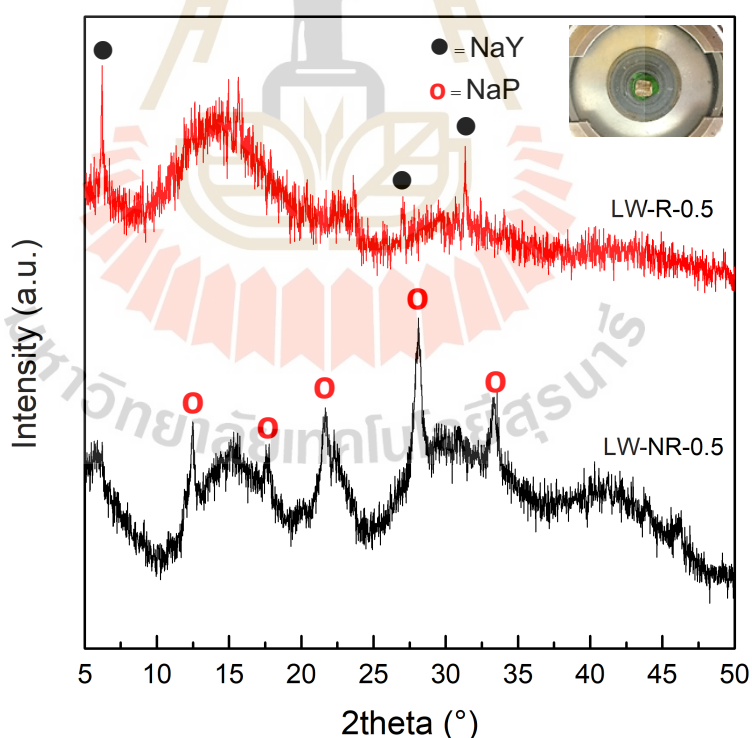
### 4.3 Effect of wood refluxing

Figure 4.7 compares the XRD pattern of LW-R-0.5 and LW-NR-0.5. As mentioned above, zeolite NaP was obtained in the non-refluxed wood from the gel of NaY. The XRD pattern of LW-R-0.5 shows peaks at 6°, 24°, and 31° which are characteristic of zeolite NaY. This result confirmed that zeolite NaY could be produced inside LW from the gel of NaY.

Figure 4.8 shows SEM images of LW-R-0.5. The particles with a size of 2  $\mu\text{m}$  was observed. These particles had polyhedral morphology similar to that of

zeolite NaY in the literature (Wittayakun et al., 2008). Last but not least, there were small particles (in red circles in Figure 4.8e and 4.8f) with octahedral morphology with a size around 1  $\mu\text{m}$ . These particles were next to the large crystals. The crystals were intergrown and built through growing phases, resulting in the larger crystals (Krisnandi et al., 2018).

Since the pore size of the refluxed sample was wider, the precursor could diffuse more easily into the middle of the wood. Therefore, water could diffuse through the middle of the wood better than the non-refluxed LW. So, the condition led to the formation of zeolite NaY.



**Figure 4.7** XRD pattern of LW-R-0.5 (red line) and LW-NR-0.5 (black line).

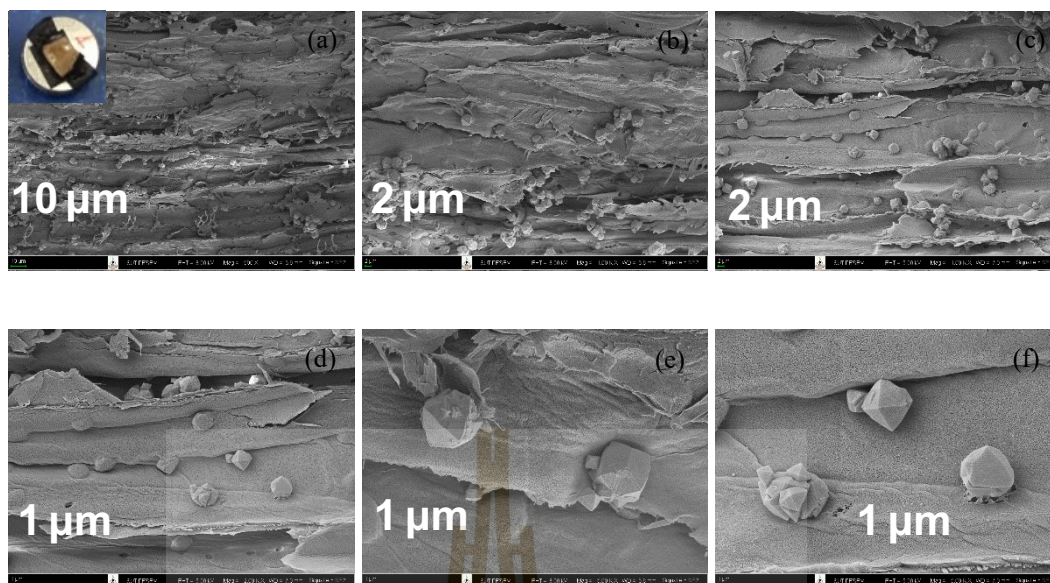


**Figure 4.8** SEM images of LW-R-0.5.

#### 4.4 Effect of sonication

The samples from sonication were characterized by XRD and SEM. Figure 4.9 shows the XRD pattern of LW-NR-So-0.5 and LW-R-So-0.5. In the case of non-refluxed sample (black line), XRD pattern shows characteristic peak of both zeolite NaP and zeolite NaY. Although the sonication was applied to the synthesis with the non-refluxed wood, it did not help much. This condition resulted in mixed zeolite phases. On the other hand, when sonication was applied to the refluxed wood, the XRD pattern of the product only shows the characteristic peaks of zeolite NaY. It is possible that the reflux cleared the pores of the wood, improving the diffusion of the precursor. The reflux might also remove particles in the pore that could be crystallization sites. However, the pore size of non-refluxed wood was still small. The precursors still could not diffuse much inside the wood.

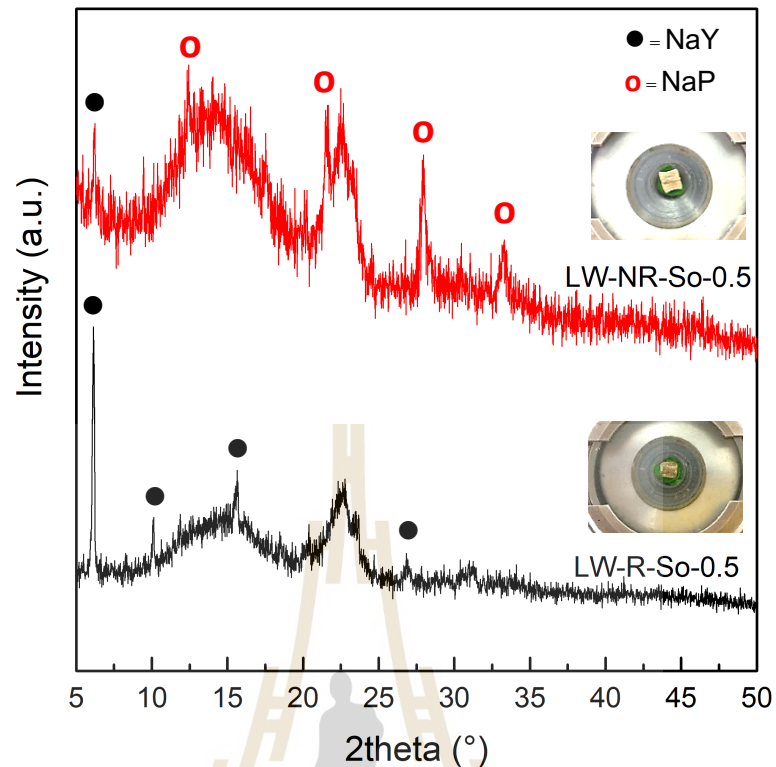


**Figure 4.9** XRD patterns of LW-NR-So-0.5 and LW-R-So-0.5.

Figure 4.10 shows the SEM image of LW-NR-So-0.5. Figures 10e and 10f are a magnified image in Figure 10c and area 2 in Figure 10d, respectively. The small particles with a size of 2-5  $\mu\text{m}$  dispersed in the pore of LW. Only spherical morphology which is characteristic of zeolite NaP was observed. Moreover, the surface inside LW of the non-refluxed sample was obviously rough which is the other components. These other components could act as amorphous particles which leads to zeolite growth (Grand et al., 2016). As before, there were smaller particles near bigger ones. The crystals were intergrown to larger phases, resulting in the bigger particles (Krisnandi et al., 2018).

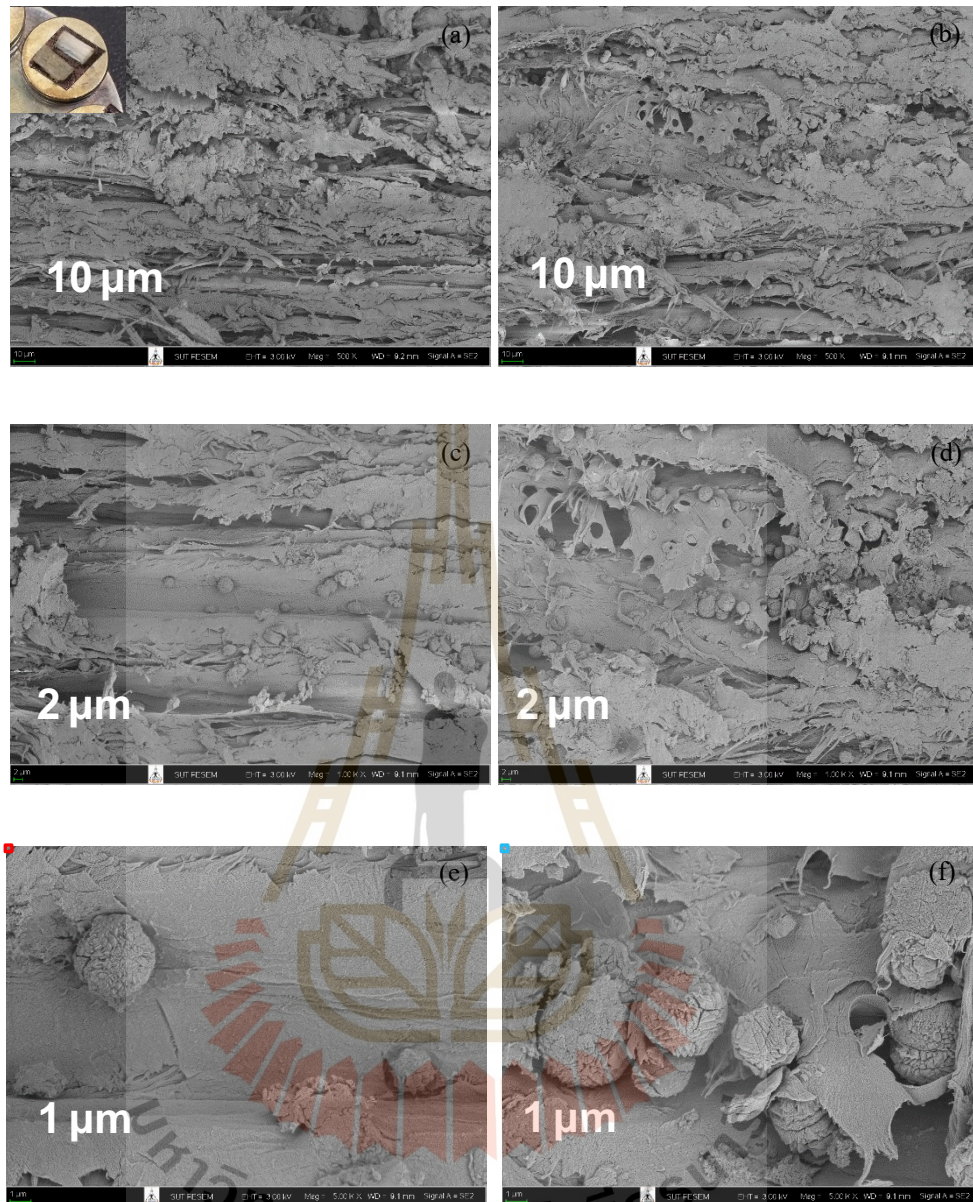


**Figure 4.10** SEM images of LW-NR-So-0.5.

Figure 4.11 shows the SEM image of LW-R-So-0.5. With the relaxed wood and sonication, the particles in the wood show polyhedral morphology with highly uniform size around 2 μm. According to XRD, these particles are zeolite NaY. Some area showed agglomerated zeolite NaY (in red circles) and some area show single

crystal zeolite NaY. Figures 11c and 11d are a magnified image of area 1 in Figure 11a and area 2 in Figure 11b, respectively. Acid refluxing could widen the pore size and without other components. Sonication could push the precursor deeper into the LW. It can be concluded that pore width expansion and sonication easily assist precursor diffusion.

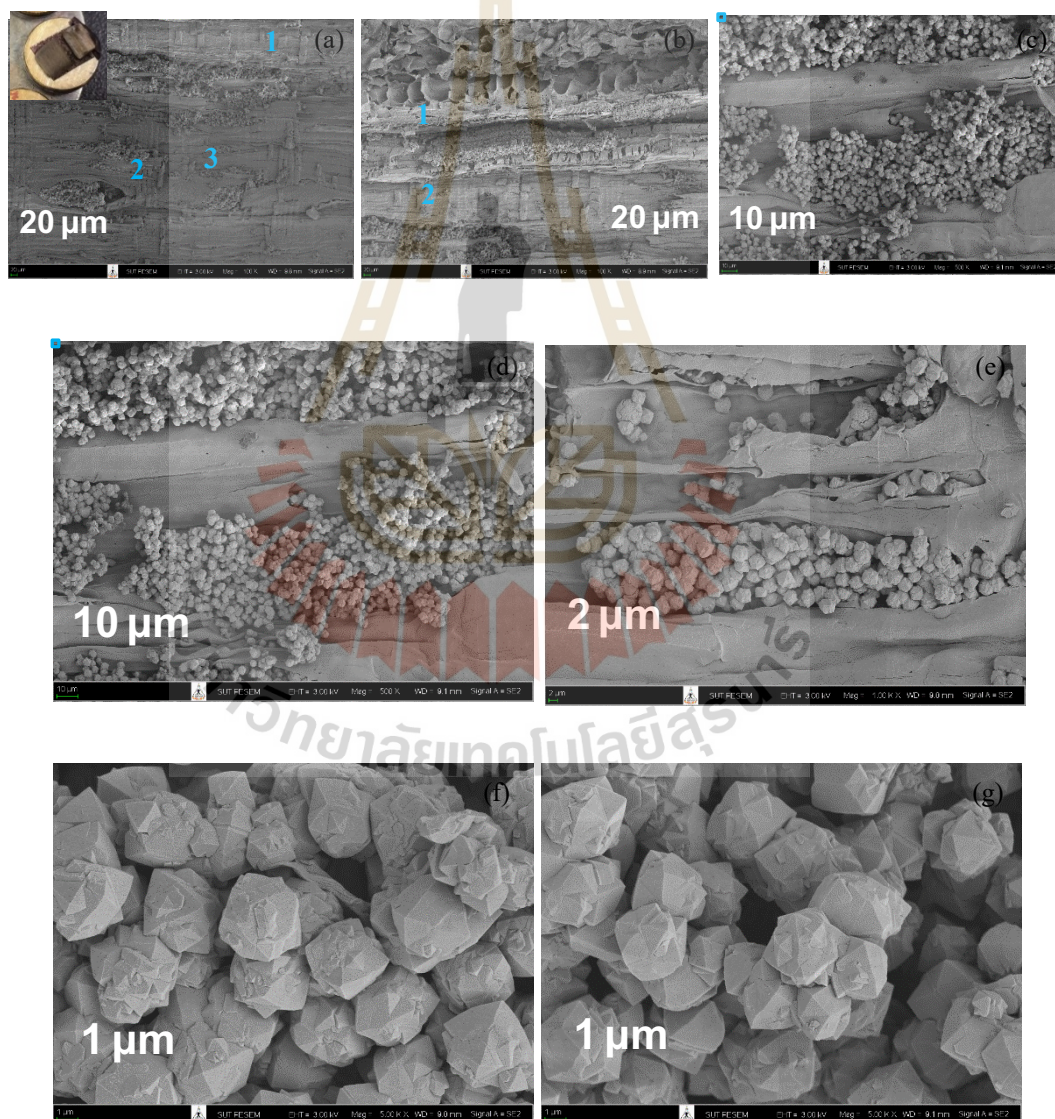
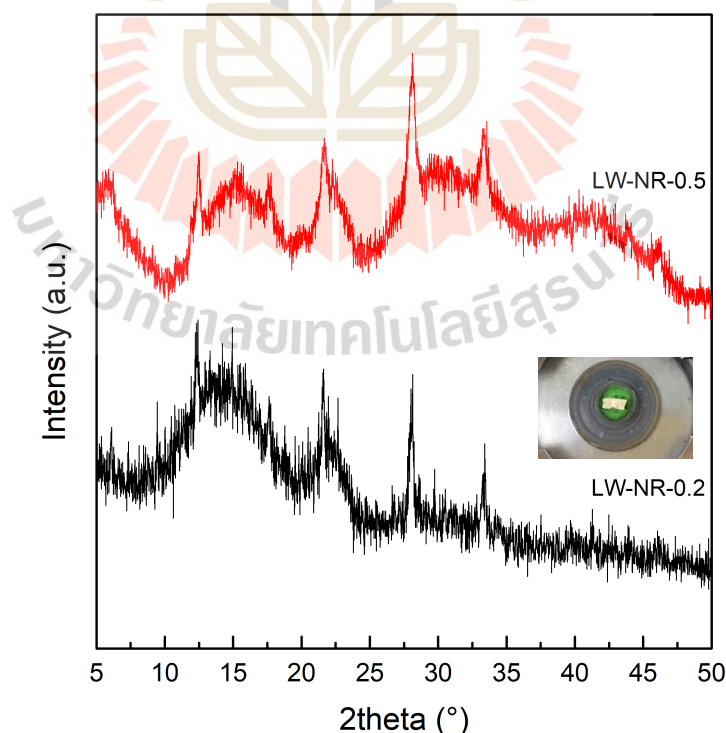


Figure 4.11 SEM images of LW-R-So-0.5.

## 4.5 Effect of wood height

Figure 4.12 shows XRD patterns of LW-NR-0.2. The inset of black line of Figure 4.12 shows LW-NR-0.2 on the XRD holder and green is plasticine. The characteristic peaks of zeolite NaP were appeared in both LW-NR-0.5 and LW-NR-0.2.

Figure 4.13 shows the SEM image of LW-NR-0.2. Only spherical morphology particles (zeolite NaP) with a size of 2-5  $\mu\text{m}$  dispersed in the pore of LW. The results of 0.2 height sample were the same a 0.5 height sample. It causes of the pore width of both samples was still the same which led to the precursor diffusion did not different. Therefore, the reaction mechanisms were still the same, results in zeolite NaP was produced in LW with the height of 0.2 cm.



**Figure 4.12** XRD pattern of LW-NR-0.5 (red line) and LW-NR-0.2 (black line).

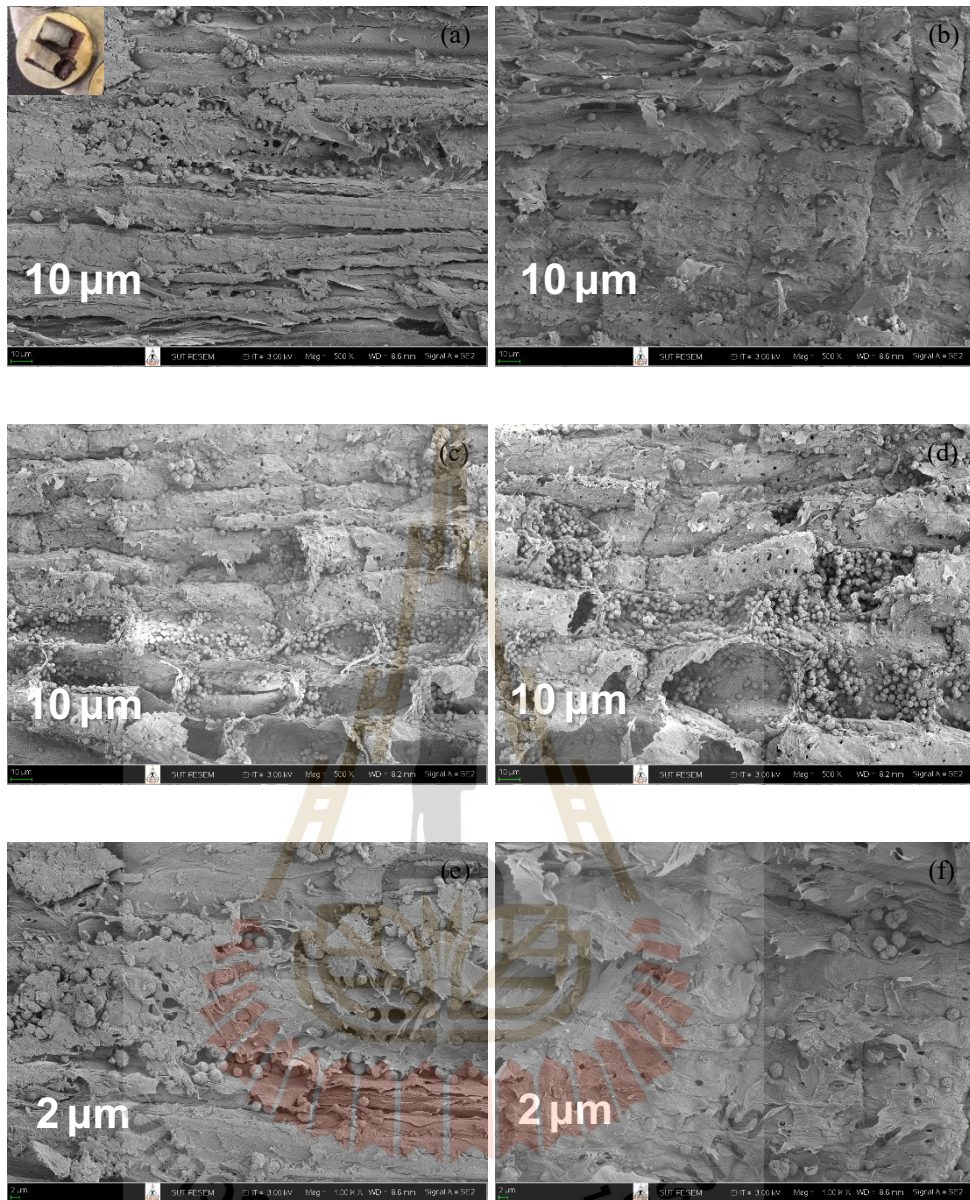
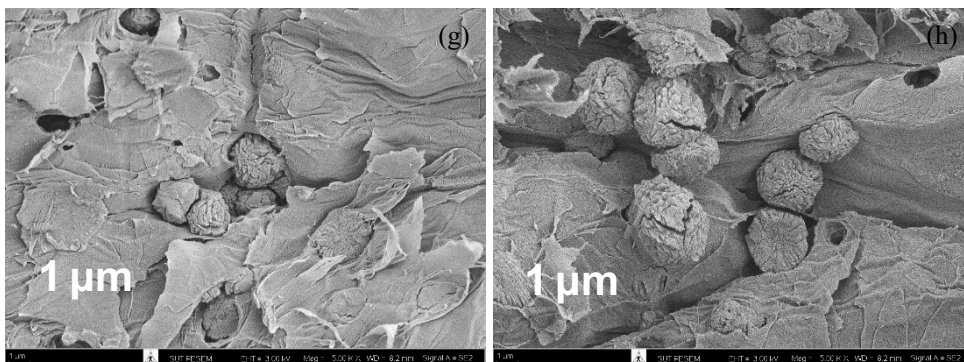


Figure 4.13 SEM images of LW-NR-0.2.



**Figure 4.13** SEM images of LW-NR-0.2 (Continued).

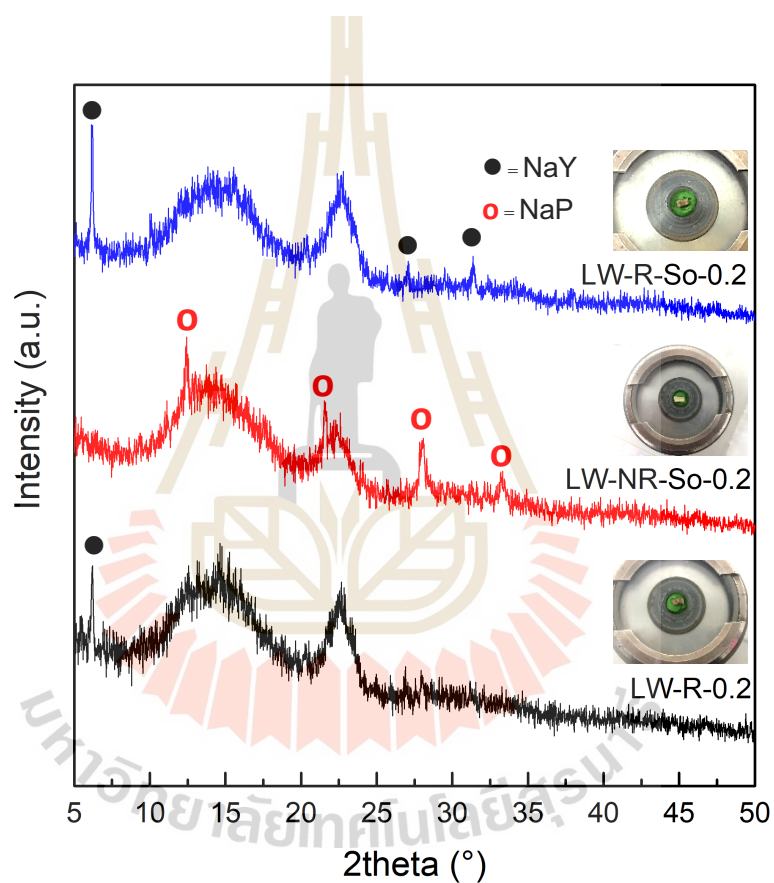
#### 4.6 Effect of wood height with wood refluxing and sonication

Figure 4.14 compares the XRD patterns of LW-R-So-0.2, LW-NR-So-0.2, and LW-R-0.2. Refluxed wood samples (LW-R-0.2 and LW-R-So-0.2) show a characteristic peak of zeolite NaY while non-refluxed sample (LW-NR-So-0.2) shows a characteristic peak of zeolite NaP.

Figures 4.15, 4.16, and 4.17 show the SEM images of LW-R-0.2, LW-NR-So-0.2, and LW-R-So-0.2, respectively. Figures 15g, 15h, and 16c are a magnified image of area 1, 2 in Figure 15d, and area red in Figure 16a, respectively. Refluxed wood samples showed polyhedral morphology while non-refluxed wood sample showed spherical morphology. Particle sizes of refluxed and non-refluxed wood samples was in the range of 1-3 and 2-5  $\mu\text{m}$ , respectively. Zeolite NaP was observed again in the non-refluxed LW even either with or without the sonication.

The results from the wood with the heights 0.2 cm (LW-NR-So-0.2 and LW-R-So-0.2) and 0.5 cm (LW-NR-So-0.5 and LW-R-So-0.5) are the same. The

samples from refluxed woods provided zeolite NaY while those from non-refluxed woods provided zeolite NaP. It could be concluded that sonication and using shorter wood height did not affect zeolite synthesis. The main effect is from wood refluxing. The expansion of pore width might assist the precursor diffusion into the wood, making the suitable condition for zeolite NaY synthesis.



**Figure 4.14** XRD pattern of LW-R-So-0.2 (blue line), LW-NR-So-0.2 (red line), and LW-R-0.2 (black line).

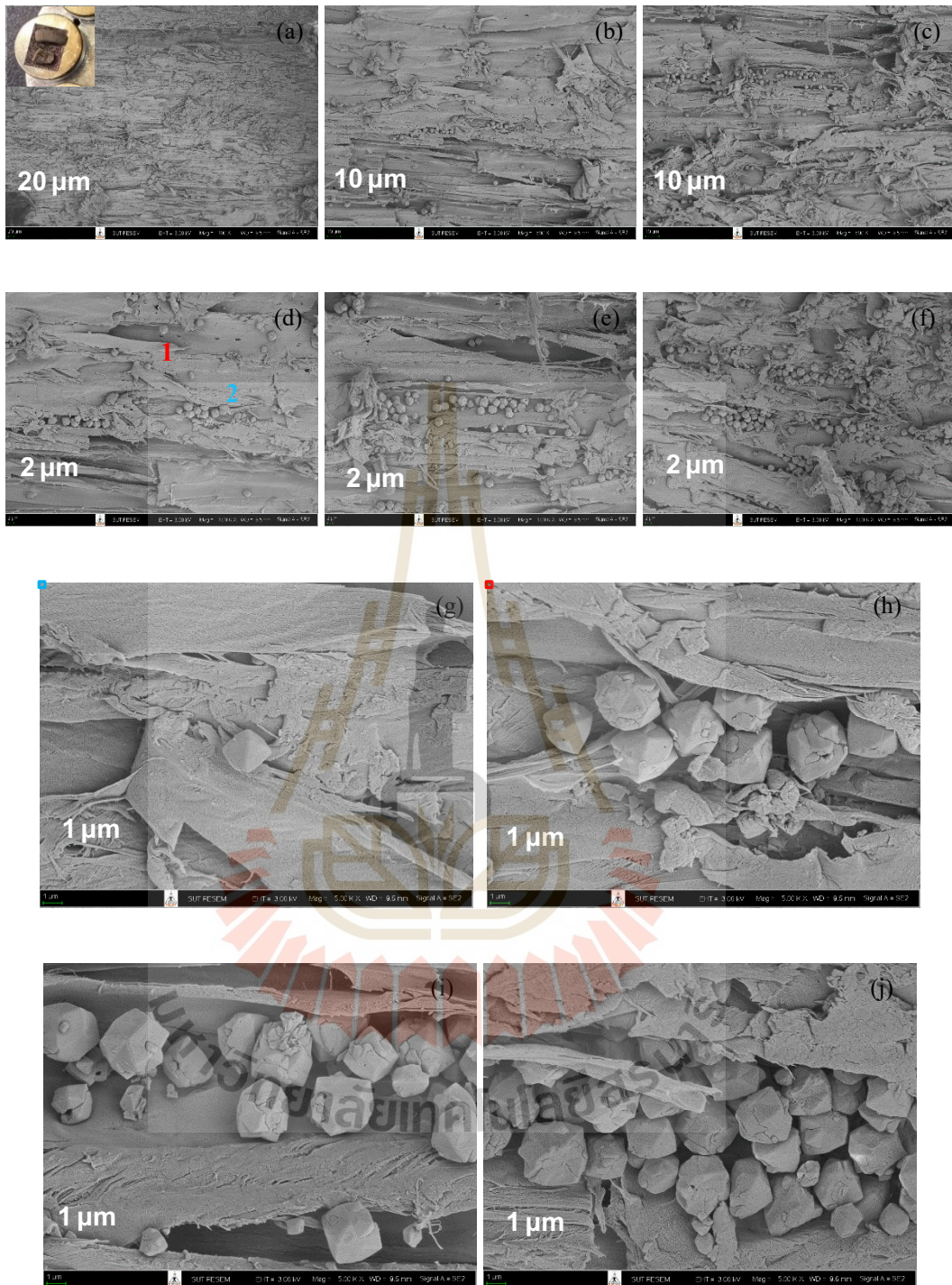


Figure 4.15 SEM images of LW-R-0.2.

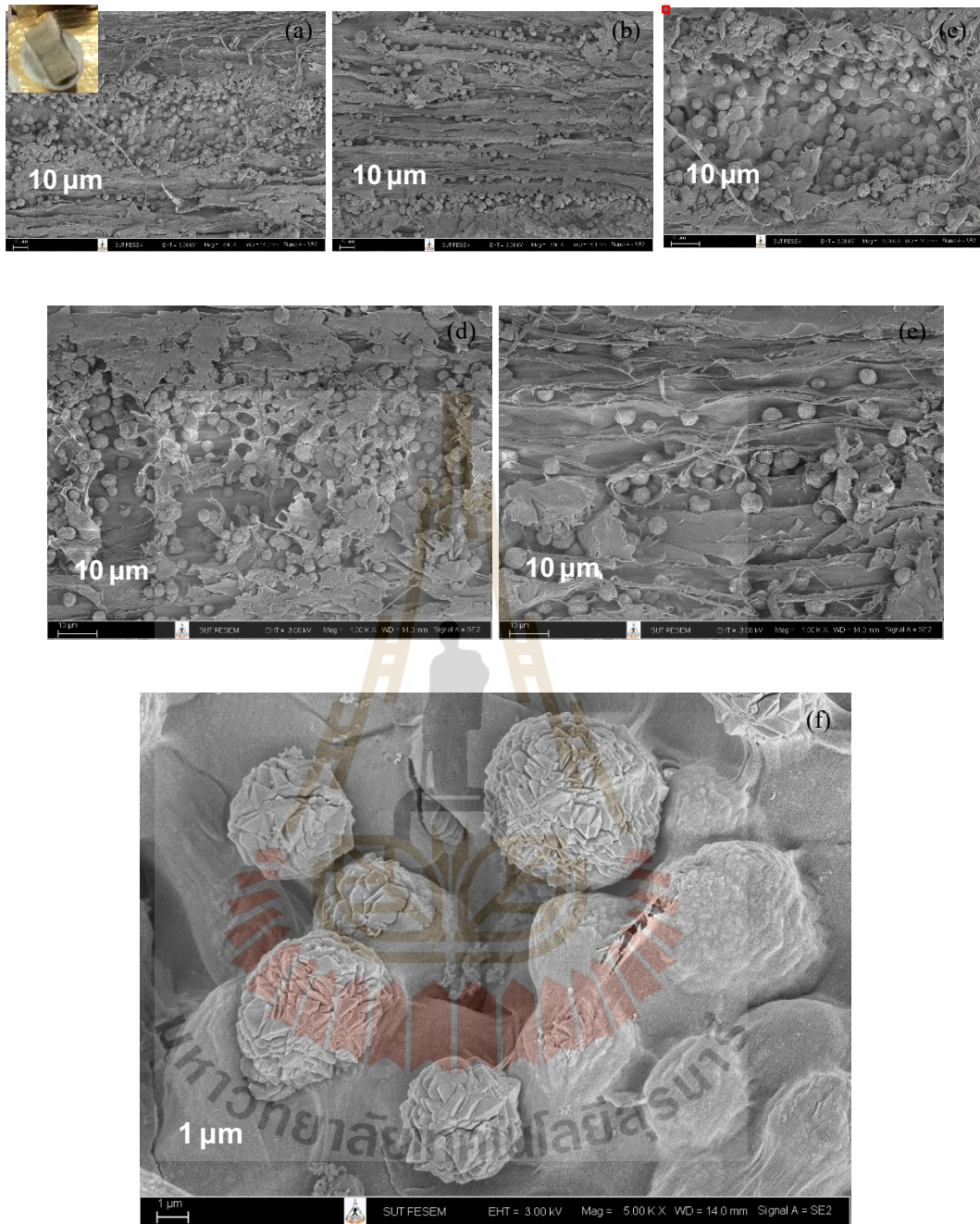


Figure 4.16 SEM images of LW-NR-So-0.2.

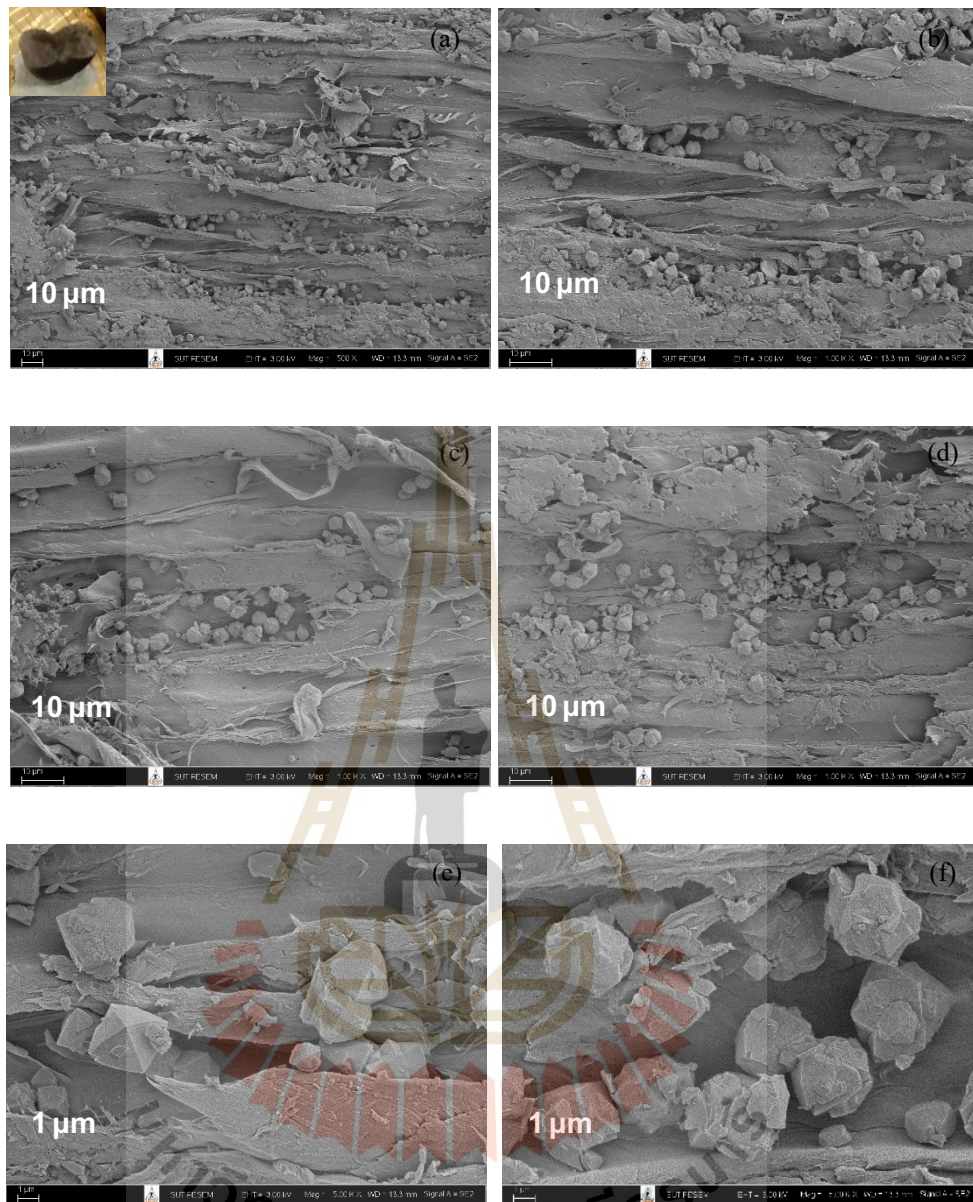


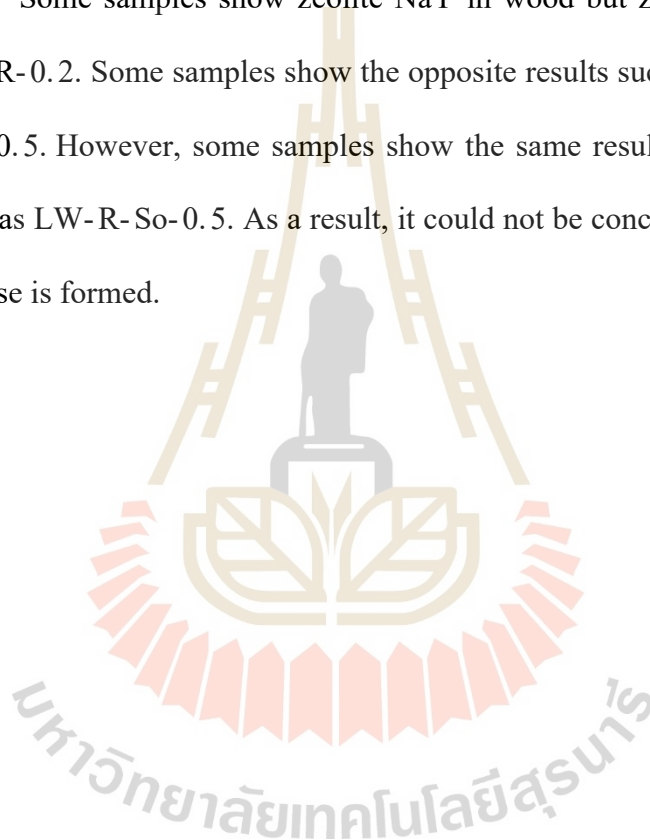
Figure 4.17 SEM images of LW-R-So-0.2.

#### 4.7 Zeolite powder outside the Lead tree wood

In addition to the wood samples, there are powders outside all the wood sample. They were characterized by XRD and SEM. Figure 4.18 shows the XRD

pattern of LW-NR-0.5, LW-R-0.5, LW-NR-So-0.5, and LW-R-So-0.5. All samples show only a characteristic peak of zeolite NaY. Figure 4.19 shows the XRD pattern of LW-NR-0.2, LW-R-0.2, LW-NR-So-0.2, and LW-R-So-0.2. LW-NR-0.2 and LW-R-0.2 show both characteristic peak of zeolite NaY and NaP while LW-NR-So-0.2 and LW-R-So-0.2 show only a characteristic peak of zeolite NaY.

Some samples show zeolite NaY in wood but zeolite NaP in powder such as LW-R-0.2. Some samples show the opposite results such as LW-NR-0.5 and LW-NR-So-0.5. However, some samples show the same results between wood and powder such as LW-R-So-0.5. As a result, it could not be concluded why NaY, NaP, or mixed phase is formed.



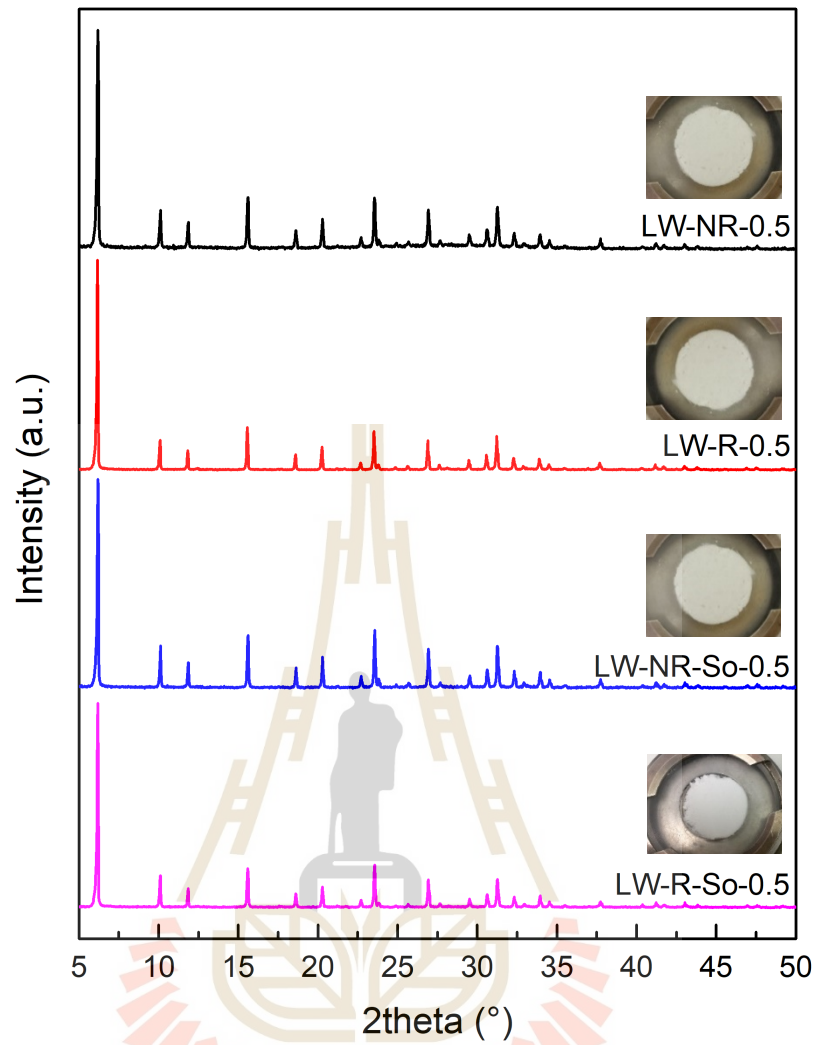


**Figure 4.18** XRD pattern of zeolite of 0.5 height powder samples outside the wood.

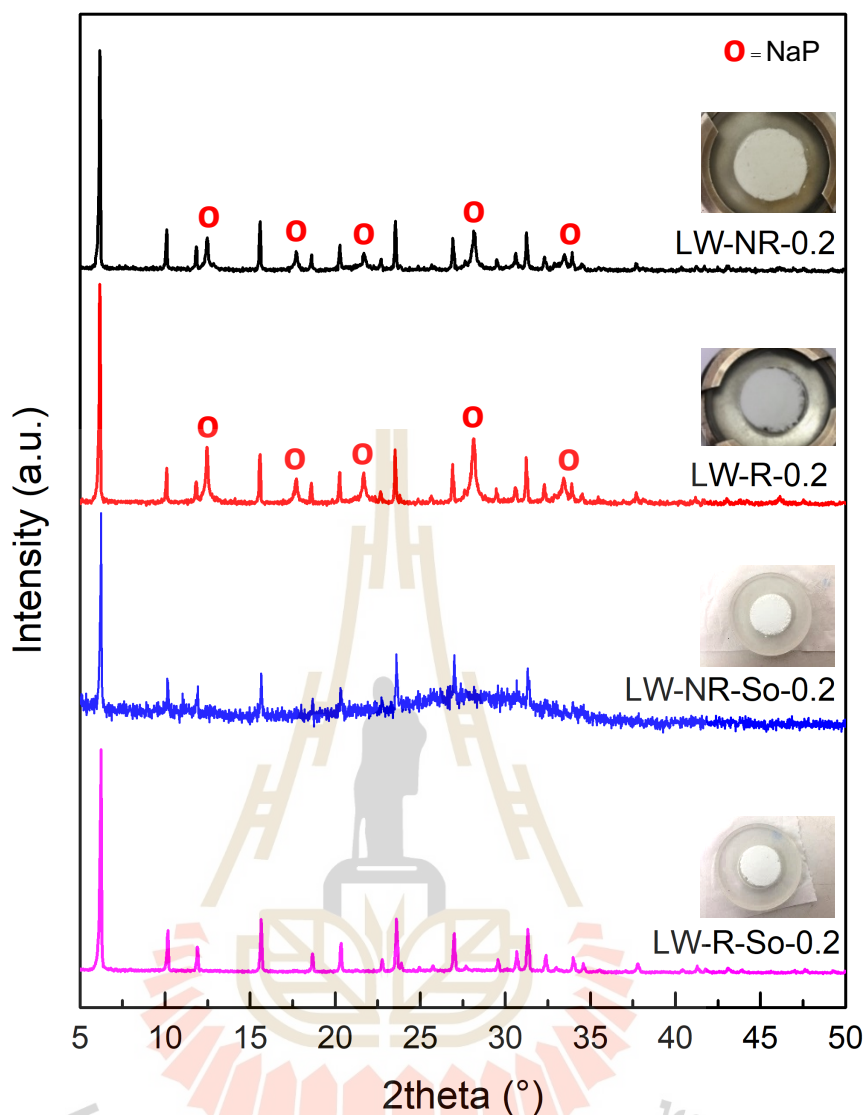


**Figure 4.19** XRD pattern of zeolite of 0.2 height powder samples outside the wood.

Figures 4.6, 4.20, 4.21, and 4.22 show the SEM images of the Pow-LW-NR-0.5, Pow-LW-R-0.5, Pow-LW-NR-So-0.5, and Pow-LW-R-So-0.5, respectively. Pow-LW-NR-0.5 (Figure 4.6) shows both polyhedral (zeolite NaY) and spherical (zeolite NaP) morphologies with the size of 2-3  $\mu\text{m}$ . However, spherical morphology appeared in a small quantity. Pow-LW-R-0.5 (Figure 4.20a) shows agglomerated

zeolite, zeolite on the wood chips (in red circles), and single crystal zeolite. Figure 4.20b-h show the polyhedral morphology with a size of 1-2  $\mu\text{m}$ . Pow-LW-NR-So-0.5 (Figure 4.21) shows only polyhedral morphology with a size of 2-3  $\mu\text{m}$ . Figure 4.21g and 4.21h shows that a very small polyhedral morphology was in the larger polyhedral morphology. This was the evidence of zeolite agglomeration. The last sample for 0.5 height, Pow-LW-R-So-0.5 (Figure 4.22) show only polyhedral morphology with a uniform size 2  $\mu\text{m}$ . Furthermore, red circles in Figure 22c-f show a small polyhedral morphology which protruded from the main crystal. This is another evidence about the zeolite agglomeration.

The SEM results of the powder were consistent with the XRD results. It seems that the applied effects do not affect the zeolite outside the wood. Owing to applying sonication, the ultrasonic radiation could disperse the precursor throughout the round bottom flask. As a result, samples with applying sonication show uniform particle size in the range of 2-3  $\mu\text{m}$ . Moreover, zeolite NaY is the main particle in samples with applying sonication. However, it could not be concluded why NaY, NaP, or mixed phase is formed.

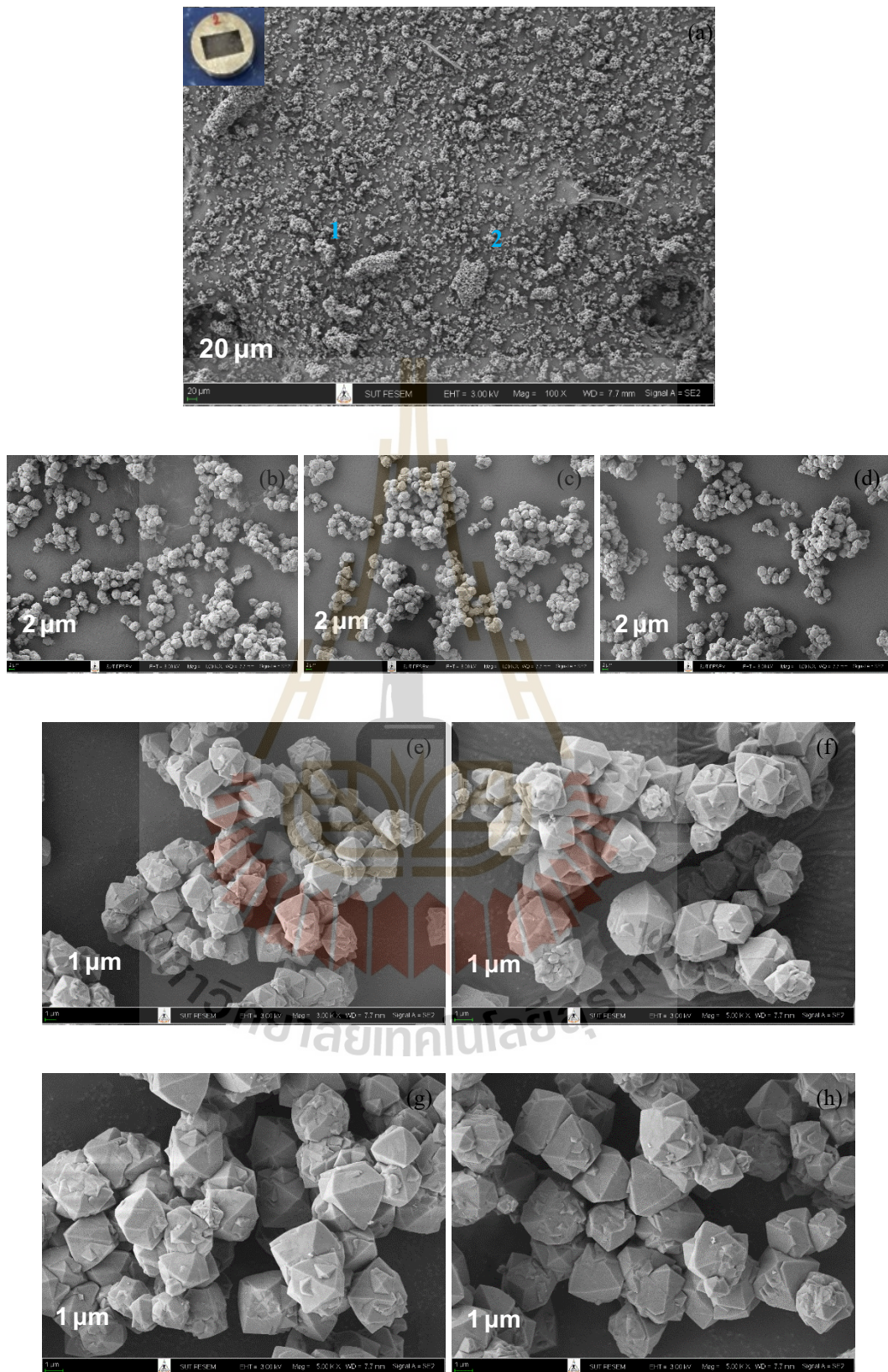
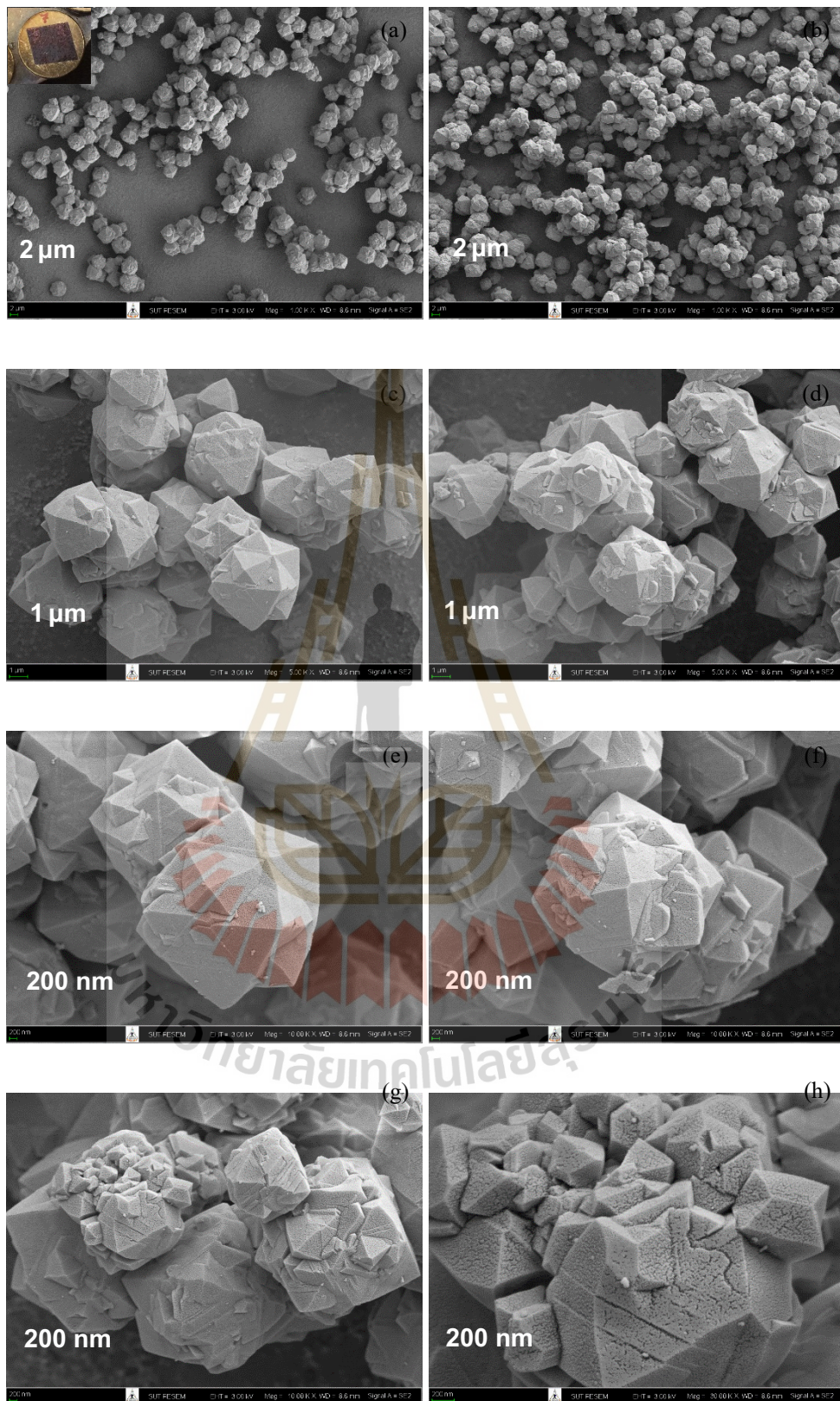
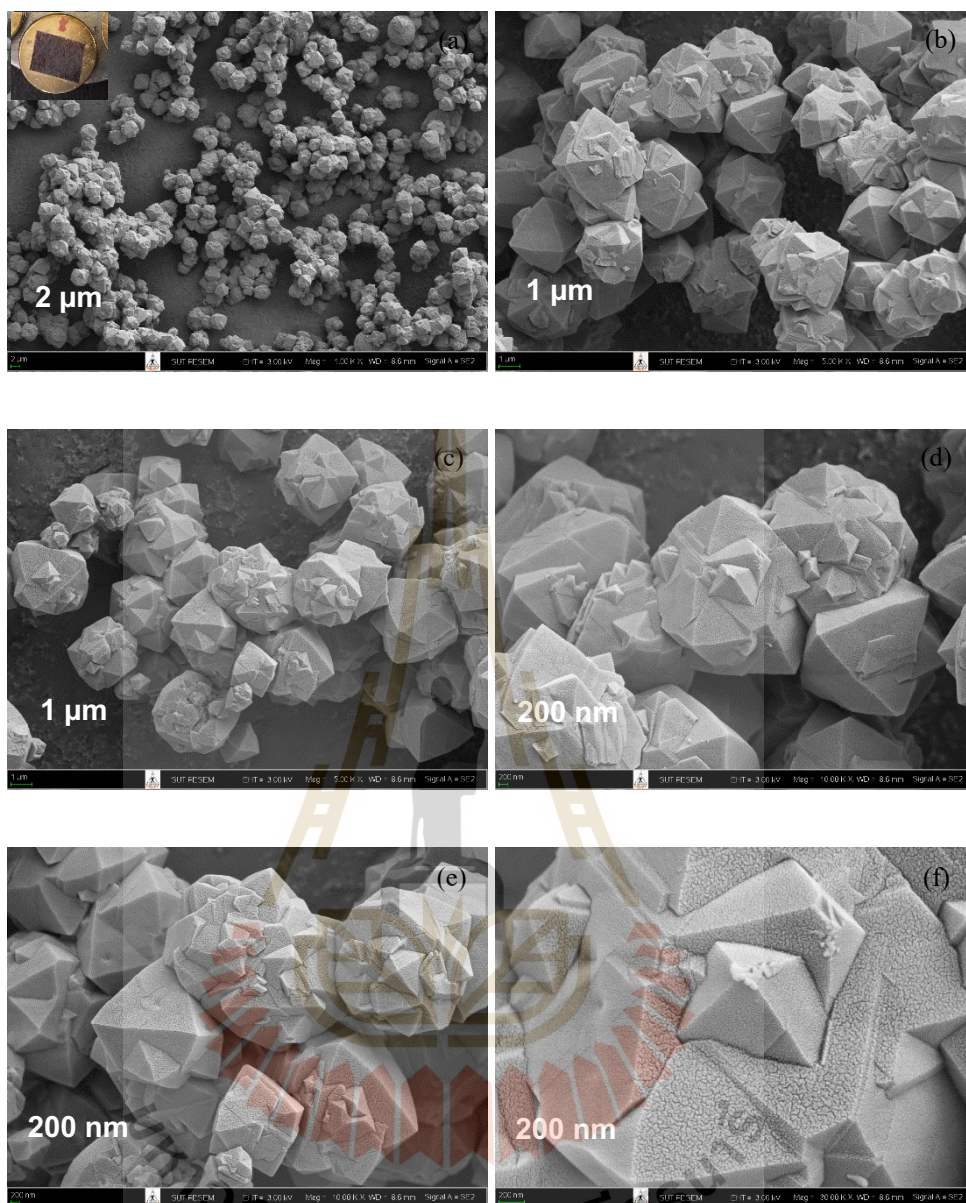


Figure 4.20 SEM images of Pow-LW-R-0.5.



**Figure 4.21** SEM images of Pow-LW-NR-So-0.5.



**Figure 4.22** SEM images of Pow-LW-R-So-0.5.

Figures 4.23, 4.24, 4.25, and 4.26 show SEM images of Pow-LW-NR-0.2, Pow-LW-R-0.2, Pow-LW-NR-So-0.2, and Pow-LW-R-So-0.2, respectively. Pow-LW-NR-0.2 and Pow-LW-R-0.2 provided the same result. Both of them show polyhedral (2-3  $\mu\text{m}$ ), spherical (2-5  $\mu\text{m}$ ), and composite zeolite between polyhedral and

spherical (2-10  $\mu\text{m}$ ) morphology, consistent with the XRD pattern. In the case of applying sonication, Pow-LW-NR-So-0.2 and Pow-LW-R-So-0.2 provided the same result. Both of them show single crystal zeolite, agglomerated zeolite, and zeolite on the wood chips. In higher magnification, polyhedral morphology which was characteristic of zeolite NaY with a size of 1-3  $\mu\text{m}$  was observed, as shown in Figure 25e and 26e. Moreover, spherical morphology which was characteristic of zeolite NaP was appeared in a small quantity, as shown in Figure 25h and 26f.

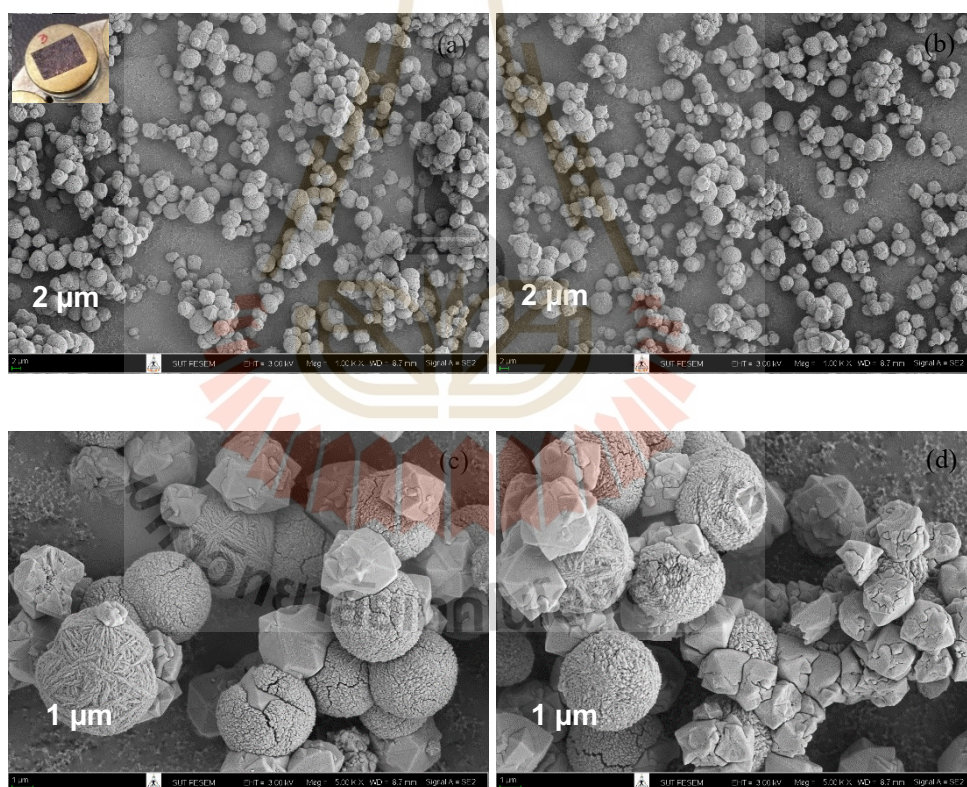


**Figure 4.23** SEM images of Pow-LW-NR-0.2.

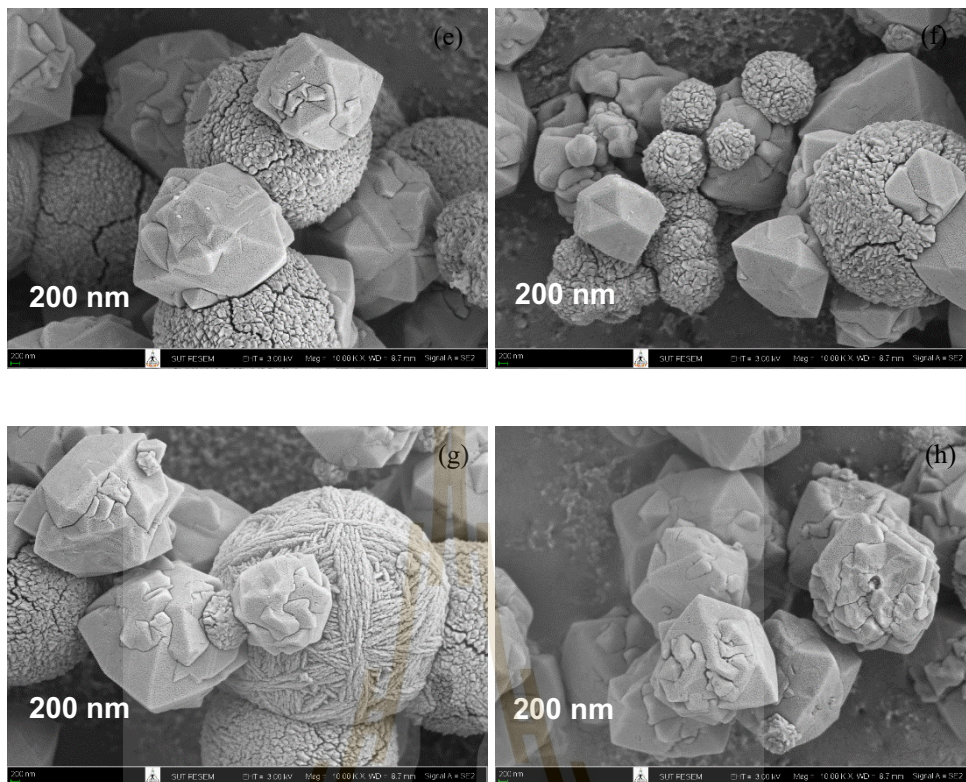


Figure 4.23 SEM images of Pow-LW-NR-0.2 (Continued).

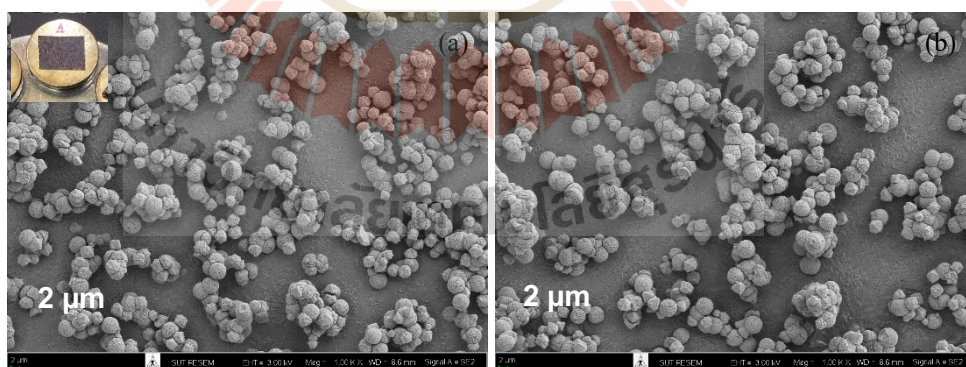


Figure 4.24 SEM images of Pow-LW-R-0.2.

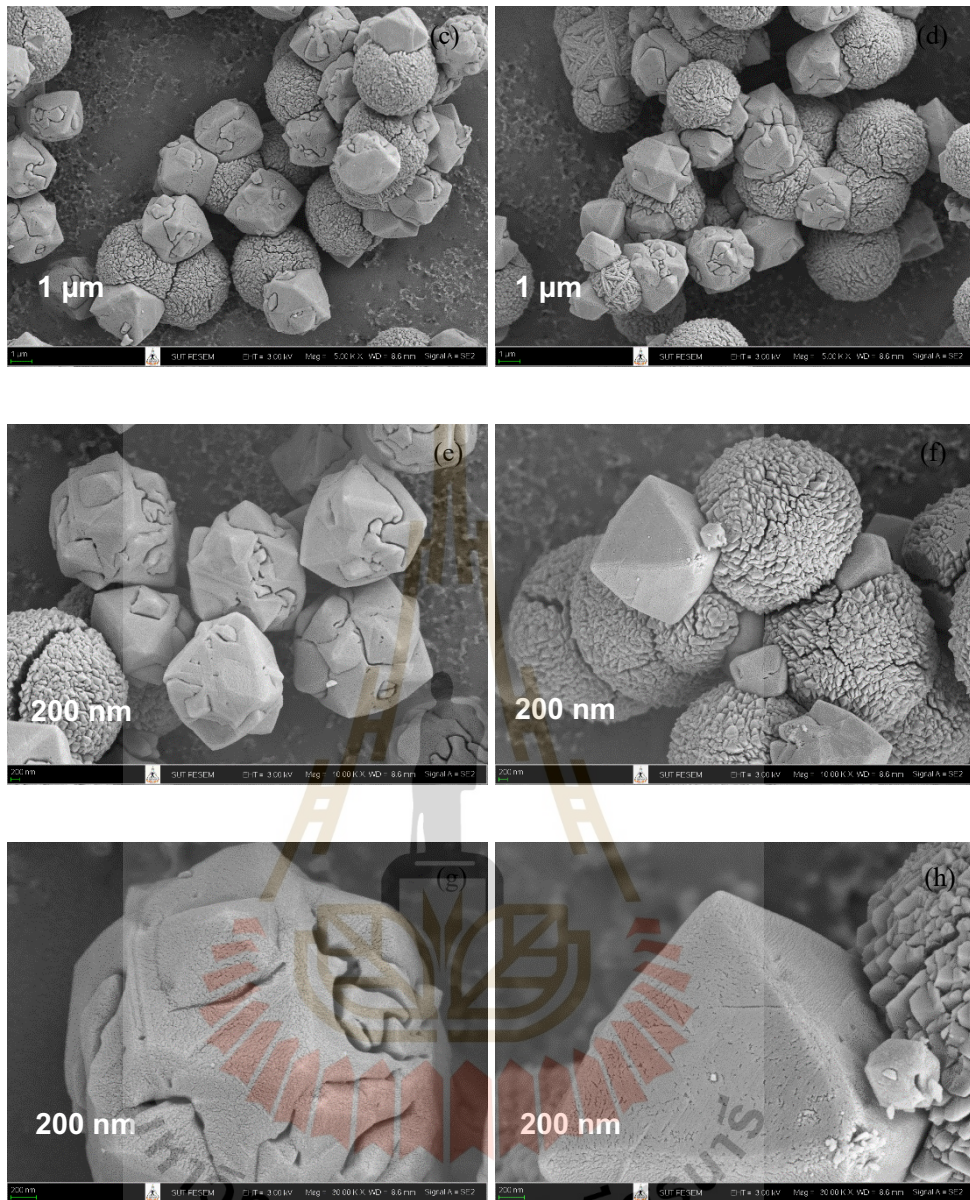


Figure 4.24 SEM images of Pow-LW-R-0.2 (Continued).

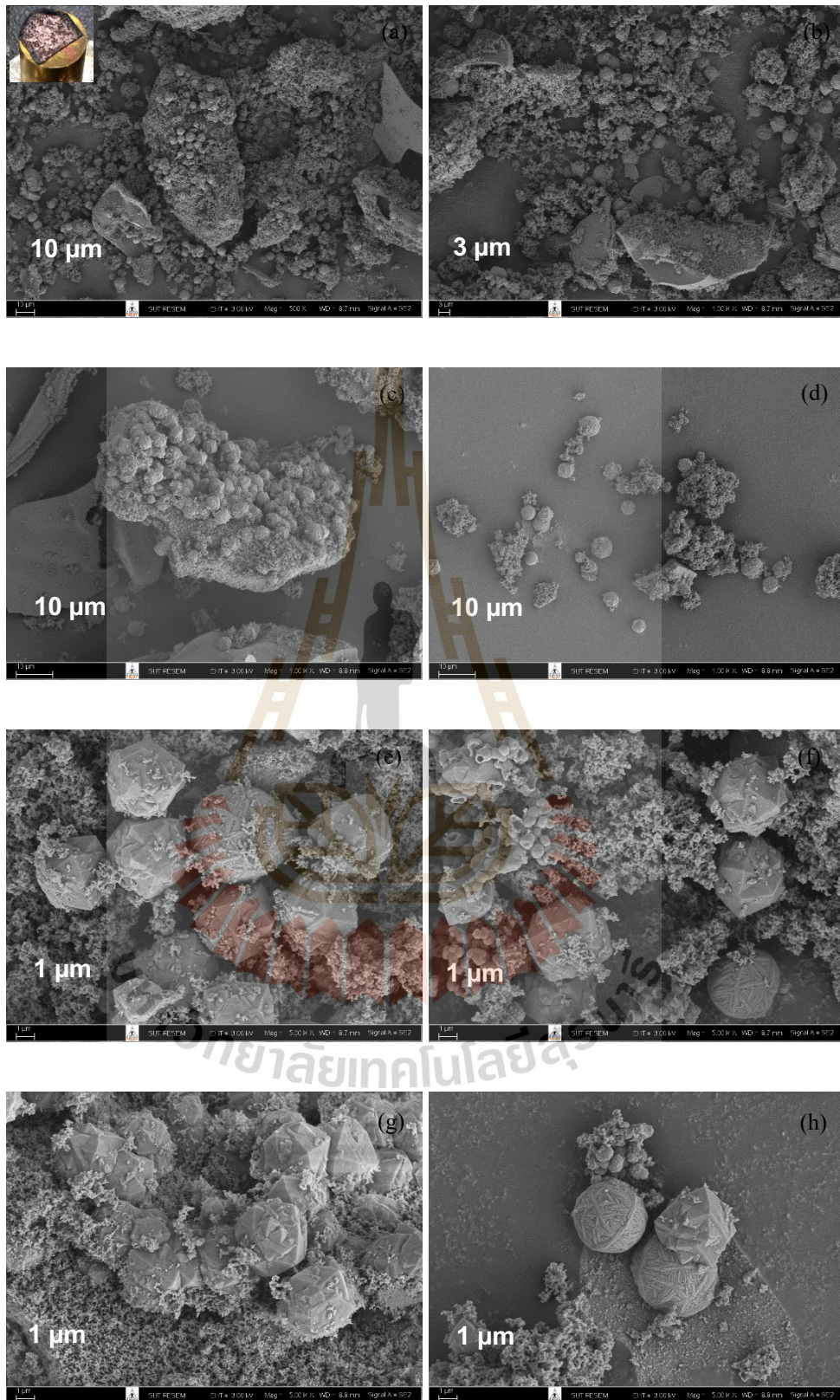
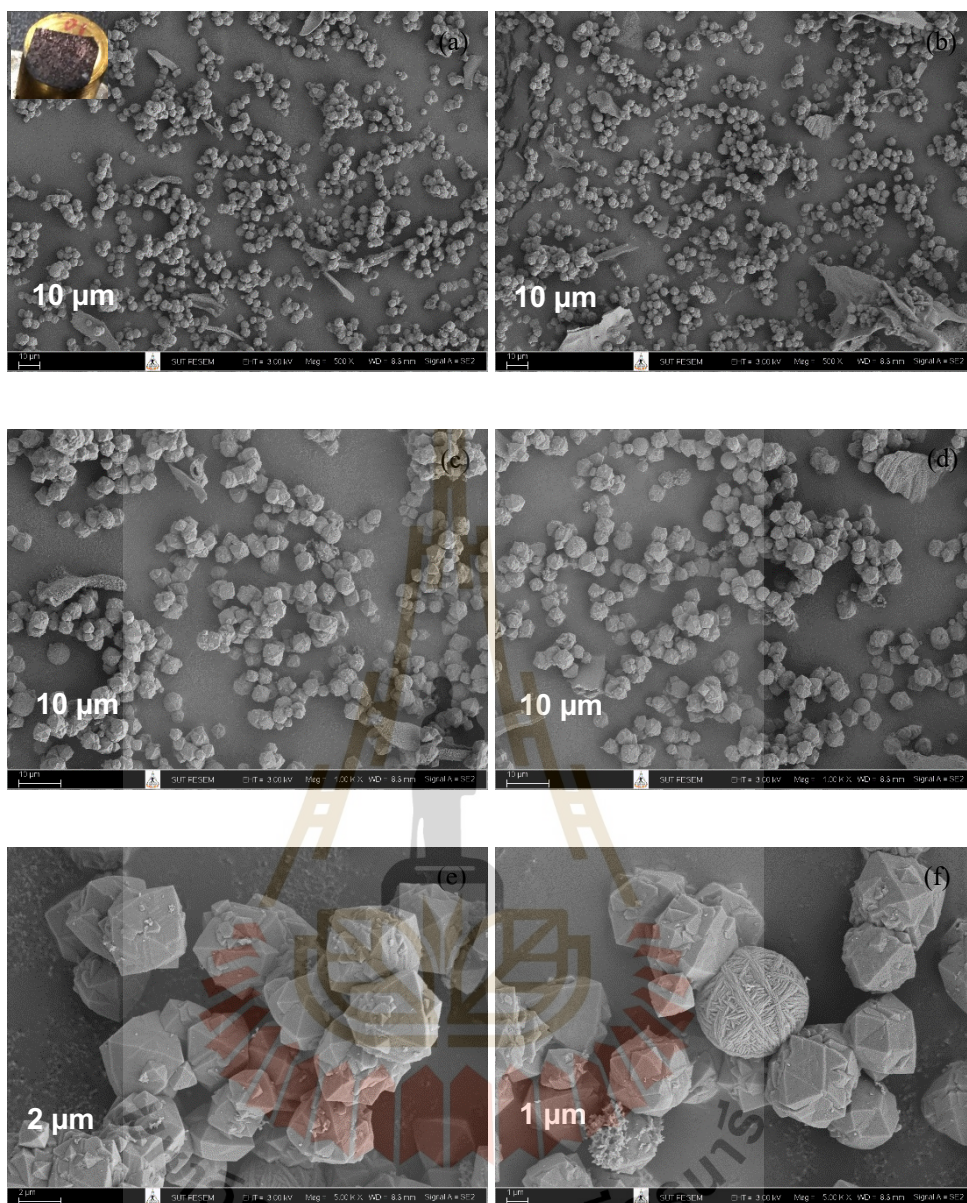


Figure 4.25 SEM images of Pow-LW-NR-So-0.2.



**Figure 4.26** SEM images of Pow-LW-R-So-0.2.

SEM images of all powder samples are summarized in Figure 4.27. In the case of 0.5 height wood samples, LW-NR-0.5 provided both spherical particles and polyhedral crystals while the rest of the samples provided only polyhedral morphology. The zeolite particle of LW-R-So-0.5 provided a uniform size of 2 μm. Moreover, all

0.2 height samples provided both spherical and polyhedral morphologies with the size of 1-3  $\mu\text{m}$ .

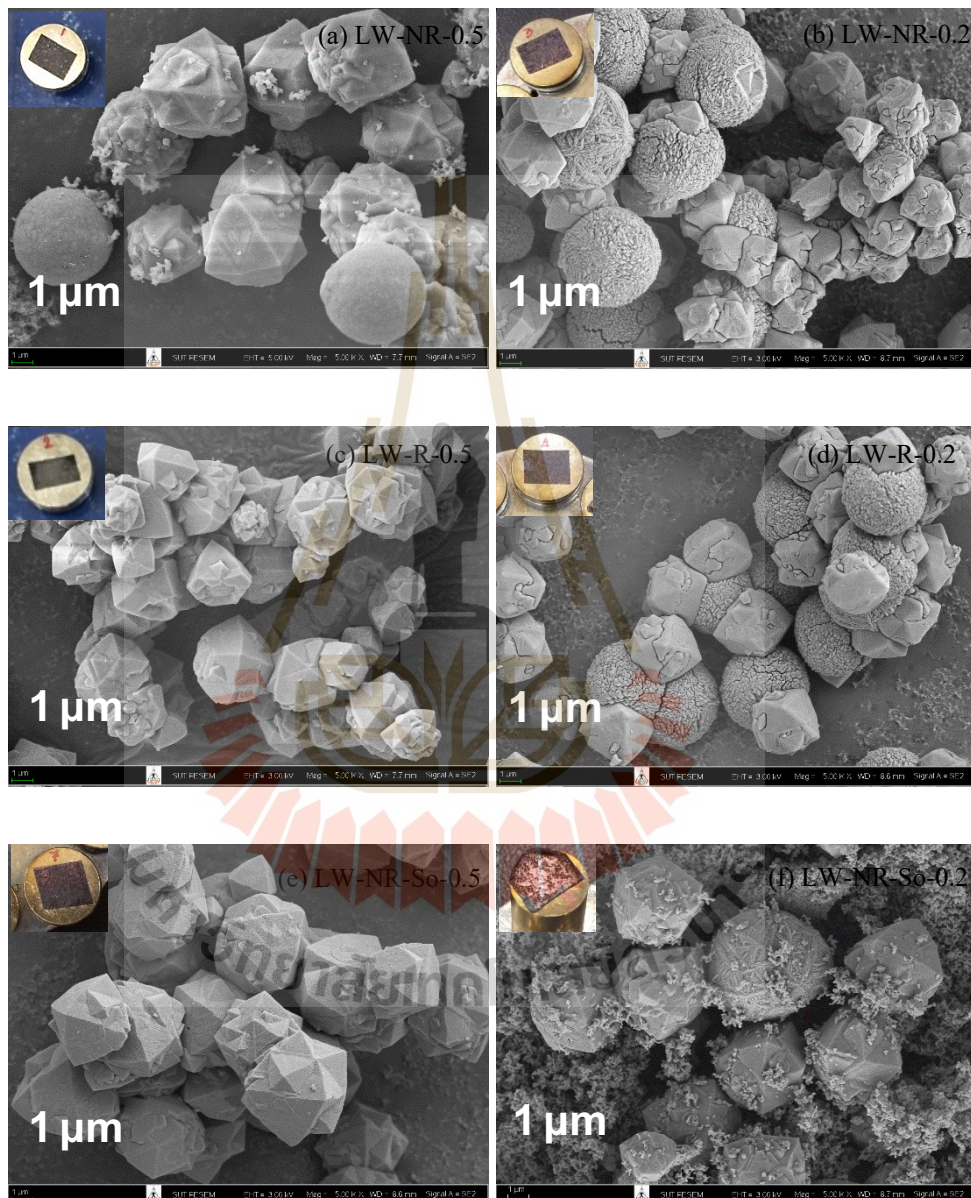


**Figure 4.27** SEM images of powder samples.

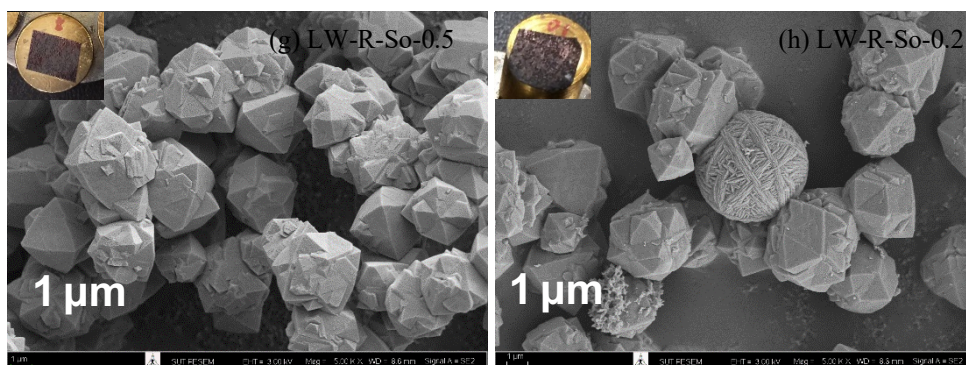


Figure 4.27 SEM images of powder samples (continued).

#### 4.8 Thermal Stability and %zeolite by TGA

Figure 4.28, 4.29, 4.30, 4.31 show TGA (a) and DTG (b) curves of 0.5 height samples, 0.2 height samples, 0.5 height powder samples, and 0.2 height powder samples, respectively. In the case of wood samples, 0.5 height samples (Figure 4.28), the first weight loss between 75 - 250°C is attributed to the loss of water. The second weight loss between 250 - 330°C is attributed to the loss of hemicellulose (Li et al., 2015). The last weight loss between 350 - 450°C is attributed to the loss of cellulose (Li et al., 2015). The remaining compounds is only zeolite about 10 - 20 %. The loss from lignin above 450°C was not observed because the wood was immersed in alkaline solution leading to delignification (Li et al., 2015). Samples with 0.2 height (Figure 4.29) provide the same result with 0.5 height wood.

In the case of powder samples outside the wood, 0.5 height samples (Figure 4.29) and 0.2 height samples (Figure 4.31), the only one weight loss between 40 - 400°C is attributed to the loss of water.

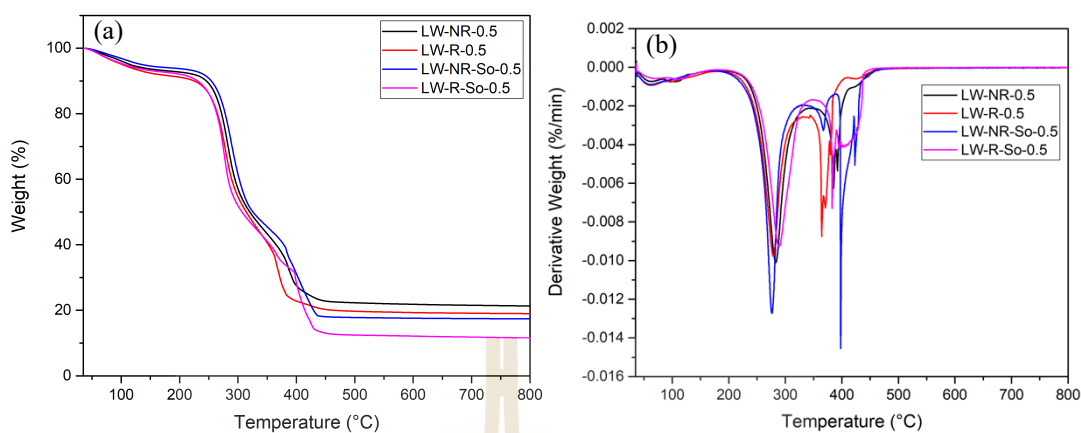


Figure 4.28 (a) TGA and (b) DTG curves of 0.5 height samples.

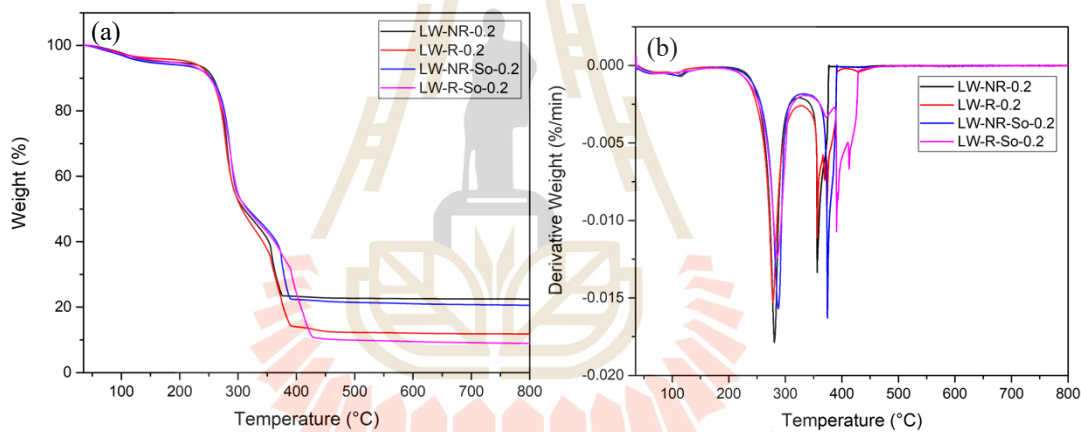


Figure 4.29 (a) TGA and (b) DTG curves of 0.2 height samples.

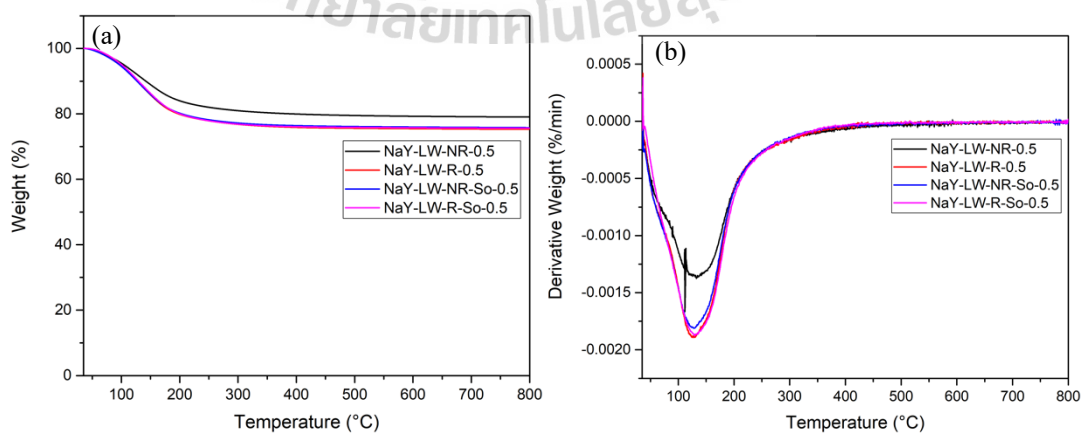
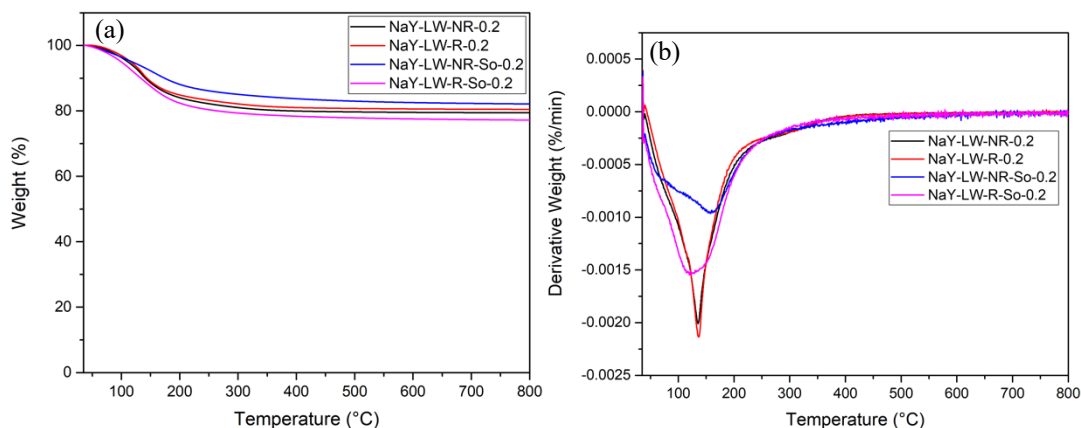


Figure 4.30 (a) TGA and (b) DTG curves of 0.5 height powder samples.



**Figure 4.31** (a) TGA and (b) DTG curves of 0.2 height powder samples.

All conditions of sample and zeolite types of product are summarized in Table 4.1. The first attempt sample is 0.5 height LW (LW-NR-0.5). Both powder and wood sample were zeolite NaP. The main proposed reason is that the gel composition in the middle of the wood is not suitable. Three methods for solving such problems are as follows: 1) wood refluxing by acid 2) reducing of wood height 3) applying sonication. After acid refluxing, zeolite NaY was synthesized. Since acid refluxing might result in pore width expansion. Therefore, the gel composition was more suitable for NaY zeolite formation than non-refluxed sample. After sonication was applied, result of non-refluxed samples was the same as refluxed sample. After reducing of the wood height, result of 0.5 height sample was the same as 0.2 height sample. Since the pore size was still the same. It means that wood refluxing is important factor for zeolite NaY synthesis. Samples with only zeolite NaY in both powder and wood samples are LW-R-So-0.5 and LW-R-So-0.2. In reality, 0.2 height wood is much harder to produce than 0.5 height wood. Cutting wood to 0.2 height wood requires more sawing power

and is very easy to break into two pieces. So, the best sample for NaY/LW synthesis is LW-R-So-0.5.

**Table 4.1** Conditions of each sample and zeolite types of product.

Sample name	Wood height (cm)	Wood refluxing	Sonication assistance	Zeolite type*	
				Powder sample	Wood sample
LW-NR-0.5	0.5	-	-	NaY + NaP	NaP
LW-R-0.5	0.5	✓	-	NaY	NaY + NaP
LW-NR-So-0.5	0.5	-	✓	NaY	NaP
LW-R-So-0.5	0.5	✓	✓	NaY	NaY
LW-NR-0.2	0.2	-	-	NaY + NaP	NaP
LW-R-0.2	0.2	✓	-	NaY + NaP	NaY
LW-NR-So-0.2	0.2	-	✓	NaY	NaP
LW-R-So-0.2	0.2	✓	✓	NaY + NaP	NaY

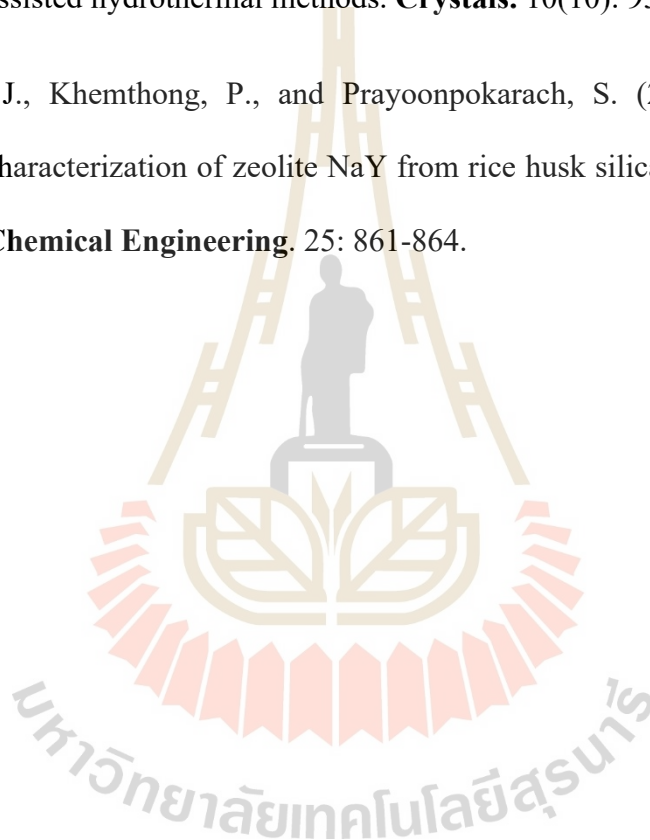
\*Zeolite type is attributed from SEM results.

## 4.9 References

- Baerlocher, Ch. and McCusker, L. (last updated 31-july-2020). Database of Zeolite Structures: <http://www.iza-structure.org/databases/>
- Grand, J., Awala, H., and Mintova, S. (2016). Mechanism of zeolites crystal growth: new findings and open questions. **CrystEngComm**. 18: 650-664.

- Hua, Z., Xu, X., Lu, Z., Song, J., He, M., Li, Z., Wang, Q., and Yan, L. (2012). Synthesis of zeolite NaP with controllable morphologies. **Microporous and Mesoporous Materials**. 158: 137-140.
- Khabuanchalad, S., Khemthong, P., Prayoonpokarach, S., and Wittayakun, J. (2008). Transformation of zeolite nay synthesized from rice husk silica to NaP during hydrothermal synthesis. **Suranaree Journal of Science and Technology**. 15(3): 225-231.
- Krisnandi, Y., Parmanti, I., Yunarti, R., Sihombing, R., and Saragi, I. (2018). Synthesis and characterization of zeolite NaY from kaolin Bangka Belitung with variation of synthesis composition and crystallization time. **Journal of Physics: Conference Series** 1095. 012043.
- Li, H., Qu, Y., and Xu, J. (2015). Microwave-assisted conversion of lignin. **Production of Biofuels and Chemicals with Microwave**. 3: 61-82.
- Li, J., Lu, Y., Yang, D., Sun, Q., Liu, Y., and Zhao, H. (2011). Lignocellulose aerogel from wood-ionic liquid solution (1-allyl-3-methylimidazolium chloride) under freezing and thawing conditions. **Biomolecules**. 12: 1860-1867.
- Pimsuta, M. (2016). **Nickel phosphide on activated carbon for hydrodeoxygenation of palm oil** (Unpublished doctor's dissertation). School of Chemistry Institute of Science Suranaree University of Technology, Nakhon Ratchasima, Thailand.

- Shirazian, S., Parto, S. G. and Ashrafizadeh, S. N. (2013). Effect of water content of synthetic hydrogel on dehydration performance of nanoporous lta zeolite membranes. **Applied Ceramic Technology**. 11: 1–11.
- Tayraukham, P., Jantarit, N., Osakoo, N., and Wittayakun, J. (2020). Synthesis of pure phase NaP2 zeolite from the gel of nay by conventional and microwave-assisted hydrothermal methods. **Crystals**. 10(10): 951.
- Wittayakun, J., Khemthong, P., and Prayoonpokarach, S. (2008). Synthesis and characterization of zeolite NaY from rice husk silica. **Korean Journal of Chemical Engineering**. 25: 861-864.



## CHAPTER V

### CONCLUSIONS

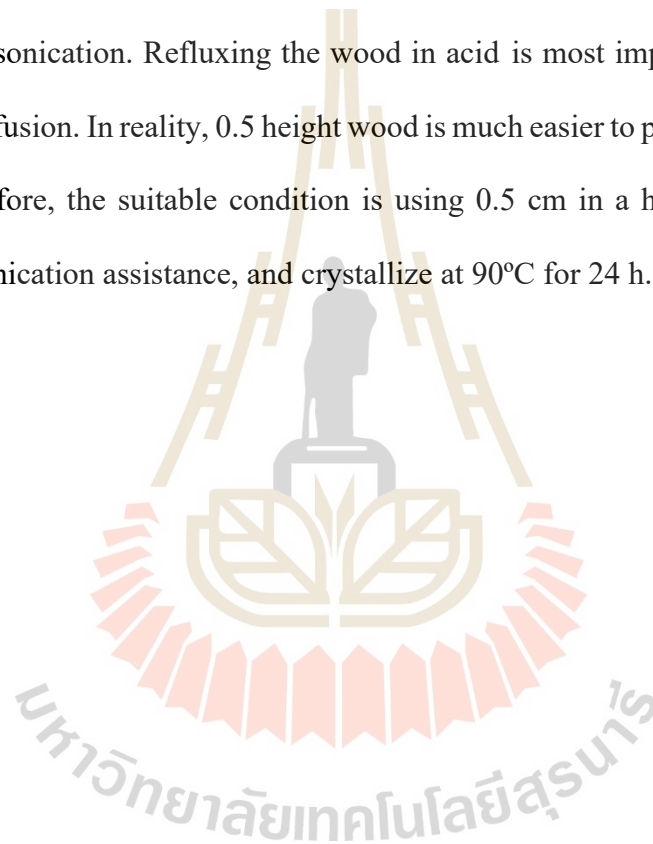
Zeolite NaY in Lead tree wood is synthesized by mixing the Lead tree wood with an overall gel of zeolite Y which has a composition with molar ratio of  $4.62\text{Na}_2\text{O} : 1\text{Al}_2\text{O}_3 : 10\text{SiO}_2 : 180\text{H}_2\text{O}$ . The XRD pattern of the untreated wood confirms the cellulose character. In the first attempt with untreated Lead tree wood (0.75 cm diameter and 0.5 cm high), the sample shows XRD pattern of zeolite NaP and cellulose. The SEM images show crystals of zeolite with spherical morphology (diameter about  $5\ \mu\text{m}$ ) in the pores of the wood. It causes of gel composition inside the Lead tree wood is not suitable for zeolite NaY synthesis. Besides the zeolite in the wood, zeolite NaY is obtained outside the wood. The crystal size is 2-3  $\mu\text{m}$  and the morphology is polyhedral.

Three effects including refluxing the wood in acid, reducing the wood height, and applying sonication are studied to improve the gel composition inside the Lead tree wood. After refluxing the wood in acid, pure phase of zeolite NaY with polyhedral morphology is successfully obtained. It causes of pore width expansion after wood refluxing about 2  $\mu\text{m}$ , results in easily diffuse precursor. Zeolite powder outside the wood is zeolite NaY with the size of 2-3  $\mu\text{m}$ .

In the case of sonicated system, non-refluxed sample provides XRD pattern of both characteristic peak of zeolite NaP and zeolite NaY while refluxed sample provides only characteristic peak zeolite NaY. It causes of the pore size is still small in non-refluxed sample. So, applying sonication does not affect to precursor diffusion.

Moreover, sonication complements the product to produce uniform zeolite NaY. Zeolite powder outside the wood is zeolite NaY with uniform size of 2  $\mu\text{m}$ .

In the case of reducing the wood height, zeolite NaP still appear because pore width is still the same. So, the synthetic mechanism is still the same. Zeolite powder outside the wood is zeolite NaP and zeolite NaY with size of 1-3  $\mu\text{m}$ . Although the height of the LW is reduced from 0.5 to 0.2 cm, the results remained the same both with and without sonication. Refluxing the wood in acid is most important factor to assist precursor diffusion. In reality, 0.5 height wood is much easier to produce than 0.2 height wood. Therefore, the suitable condition is using 0.5 cm in a height wood with acid refluxing, sonication assistance, and crystallize at 90°C for 24 h.



# CURRICULUM VITAE

## Panot Krukkratoke

**Address** D501 Suranivet 13 Dormitory, Suranaree university, 111, Maha  
Witthayalai Rd, Suranari, Mueang Nakhon Ratchasima District,  
Nakhon Ratchasima 30000 Email: notzsone@gmail.com

### Education

2015 B.Sc. (Chemistry) with first class honors  
Suranaree University of Technology (SUT), Nakhon  
Ratchasima, Thailand

2019 - 2020 Student in M.Sc. program in Chemistry, SUT

### Scholarship

2019 - 2020 Thailand Graduated Institute of Science and Technology  
(TGIST, Contact No. SCA-CO-2562-9802-TH)